Ann. Inst. Henri Poincaré Comb. Phys. Interact. 1 (2014), 265–306
DOI 10.4171/AIHPD/8

On the two-point function of general planar maps and hypermaps

Jérémie Bouttier, Éric Fusy,[1] and Emmanuel Guitter

Abstract. We consider the problem of computing the distance-dependent two-point function of general planar maps and hypermaps, i.e., the problem of counting such maps with two marked points at a prescribed distance. The maps considered here may have faces of arbitrarily large degree, which requires new bijections to be tackled. We obtain exact expressions for the following cases: general and bipartite maps counted by their number of edges, 3-hypermaps and 3-constellations counted by their number of dark faces, and finally general and bipartite maps counted by both their number of edges and their number of faces.

Mathematics Subject Classification (2010). Primary 05; Secondary 52, 60, 82.

Keywords. Random geometry, maps, graph distance, two-point function, discrete integrability, bijections, enumerative combinatorics.

Contents

1. Introduction

Much attention has been devoted to the study of metric properties of random planar maps, starting from the physical predictions of Ambjørn and Watabiki [2] and the seminal probabilistic work of Chassaing and Schaeffer [10]. Of particular interest

[1]The work of Jérémie Bouttier and Éric Fusy was partly supported by the ANR projects "Cartaplus" 12-JS02-001-01.

is the so-called two-point function which, colloquially speaking, encodes the distribution of the distance between two random points in a random map. This two-point function has been computed exactly [5], [12] for several families of maps: quadrangulations, triangulations, Eulerian triangulations... A general formalism was developed in [8] to address the case of maps with controlled face degrees but, in practice, a fully explicit expression was only obtained in the case of bounded face degrees. In this paper, we consider instead families of maps with *unbounded* face degrees: general (arbitrary) planar maps, bipartite planar maps and, more generally, hypermaps and constellations. The control is then on their natural size parameter, namely their number of edges. We will compute exactly the two-point function of these maps, using as a new ingredient some bijections which relate them to maps with bounded degrees, and keep track of distances (in the case of hypermaps, we actually consider a "quasi-distance" based on oriented edges). The two-point function of general maps was obtained recently by Ambjørn and Budd [1], using a distance-preserving bijection with planar quadrangulations. Here we shall extend their bijection and get a correspondence between, on the one hand, bipartite maps with controlled face degrees and, on the other hand, hypermaps with controlled hyperedge degrees but arbitrary (uncontrolled) face degrees. Briefly said, the Ambjørn-Budd bijection consists in applying on quadrangulations the rules opposite to those used for the Schaeffer bijection [10], [16] and here we shall apply the same trick to the more general rules used for the BDG bijection [7].

The paper is organized as follows. All the necessary bijections are established in Section 2 (Figure 1 provides an overview intended to help the reader). We start by introducing so-called suitably labeled maps and well-labeled hypermaps (Section 2.1) and a very general bijection Φ between them, using the BDG rules (Section 2.2). Reversing these rules gives rise to another "mirror" bijection Φ^- (Section 2.3). We will then specialize Φ and Φ^- to vertex-pointed bipartite maps endowed with their geodesic labeling (Section 2.4): Φ yields the BDG bijection, Φ^- is the new ingredient mentioned above, and their composition yields a direct distance-preserving correspondence between hypermaps and mobiles. We then discuss the further specialization to constellations (Section 2.5), before completing some technical proofs (Section 2.6) and discussing the extension to maps of higher genus (Section 2.7). In Section 3, we apply these bijections to compute explicitly the two-point function of several families of maps controlled by their number of edges: general maps (Section 3.1), bipartite maps and general hypermaps (Section 3.2), 3-hypermaps (Section 3.3) and 3-constellations (Section 3.4). Connections to previous works [5], [12], and [8] are discussed where applicable. In Section 4, we provide a refinement of the two-point function of general maps (Section 4.1) and bipartite maps (Section 4.2), where we control both their number of edges and their number of faces. We conclude in Section 5 by some remarks and open questions.

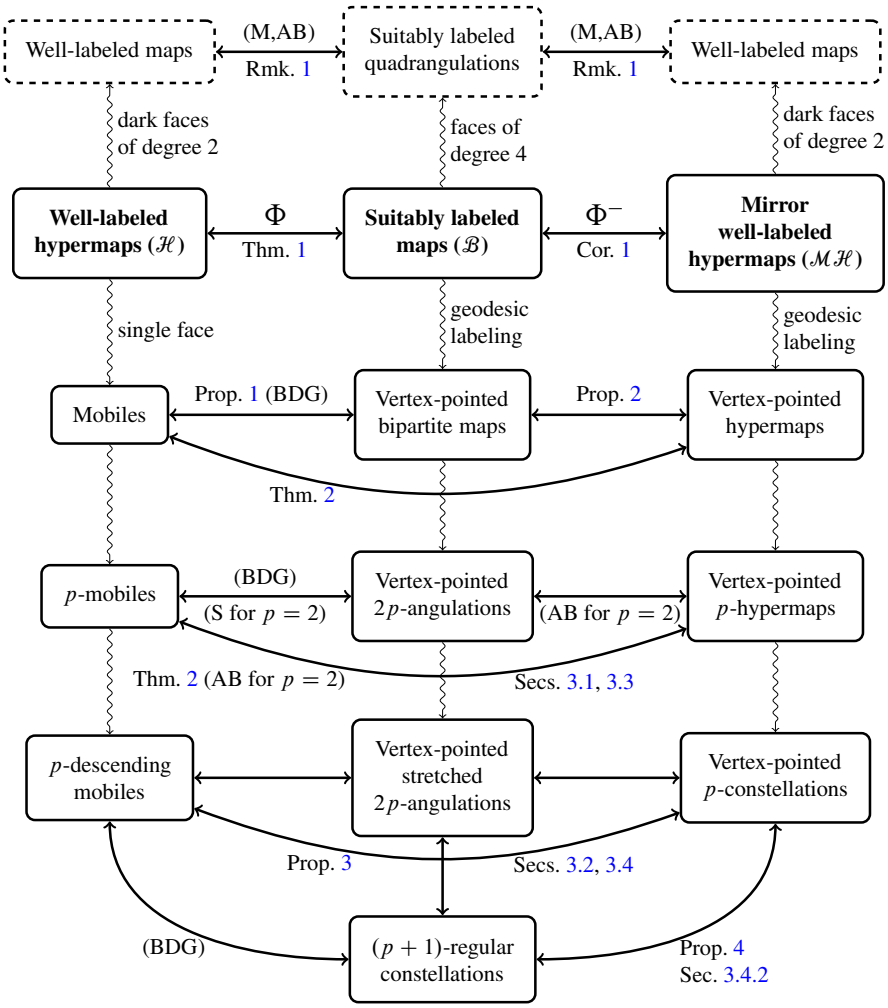

Figure 1. An overview of the bijections presented in Section 2. Bijections are represented by lines with double arrows and wiggled lines represent specializations. Where applicable, we refer to the text (i.e., to the statements in Section 2 and to the applications in Section 3) or to previous works: S stands for the Schaeffer bijection [16], BDG for the bijection of [7], M for the Miermont bijection [14] and AB for bijections introduced in [1]. (Note that the (M,AB) bijections on the first line specialize to the those on the fourth line for $p = 2$, the corresponding wiggling lines are not displayed to avoid overloading the figure.)

2. Bijections

2.1. Suitably labeled maps and well-labeled hypermaps: definitions. A *suitably labeled map* is a map B (on the sphere) where each vertex v carries a label $\ell(v) \in \mathbb{Z}$, such that, for any edge e of B with endpoints u and v, we have $|\ell(v)-\ell(u)| = 1$. Note that B is necessarily bipartite (each edge connects a vertex of odd label to a vertex of even label). A *local max* (resp. *local min*) is a vertex such that all neighbors have smaller (resp. greater) label. The *cw-type* (resp. *ccw-type*) of a face f is the cyclic list of integers given by the labels of vertices in clockwise (resp. counterclockwise) order around f. Denote by $\mathcal{B}$ the set of suitably labeled maps.

An Eulerian map is a map (on the sphere) with all vertices of even degree; such maps can be properly bicolored at their faces (with dark faces and light faces), i.e., such that any edge has a dark face on one side and a light face on the other side. A *hypermap* H is a properly face-bicolored Eulerian map (viewing dark faces as hyperedges). The *star-representation* of H is the bipartite map S obtained by replacing the contour of each dark face f (of a given degree d) by a star (of degree d) centered at a new black vertex v_f placed inside f, see Figure 2.

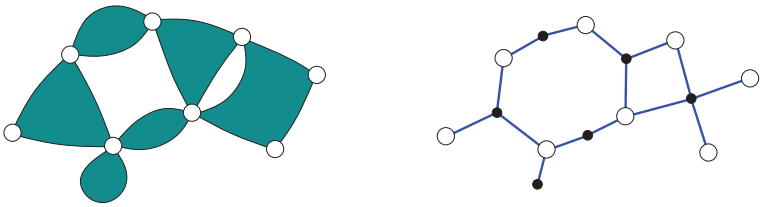

Figure 2. Left: a hypermap; right: its star-representation.

A *well-labeled hypermap* is a hypermap H (on the sphere) where each vertex v carries a label $\ell(v) \in \mathbb{Z}$ such that, for any edge e incident to v, with the dark face incident to e on the right of e traversed from v to its other endpoint u, we have $\ell(u) \geq \ell(v) - 1$. For a vertex u of H, a *right neighbor* of u is a vertex v adjacent to u, and such that there exists an edge from v to u with a dark face on its right. A *right local min* (resp. *right local max*) of H is a vertex u such that any right neighbor v of u satisfies $\ell(v) \geq \ell(u)$ (resp. $\ell(v) \leq \ell(u)$). The *cw-type* τ of a dark face f is the cyclic list of integers given by the labels of vertices in *clockwise* order around f. Denote by $\mathcal{H}$ the family of well-labeled hypermaps. Note that by definition, the cw-type τ of a dark face is a so-called *Łukasiewicz cyclic sequence*, i.e., a cyclic integer list such that the difference between an element of the list and the preceding one is at least -1. Define the *upper completion* $c^{\uparrow}(\tau)$ (resp. *lower completion* $c^{\downarrow}(\tau)$) of τ as the cyclic sequence obtained from τ by inserting the rising sequence $i+1, \ldots, j+1$ (resp. the rising sequence $i-1, \ldots, j-1$) between any two consecutive elements i, j such that $j \geq i$. The *upper complement* $\overline{\tau}^{\uparrow}$ (resp. *lower complement* $\overline{\tau}^{\downarrow}$) of τ is

the cyclic sequence $c^{\uparrow}(\tau)\backslash\tau$ (resp. $c^{\downarrow}(\tau)\backslash\tau$) taken in reverse order, see Figure 3 for an example. Note that the upper or lower complement is also a Łukasiewicz cyclic sequence, and that the mappings from a Łukasiewicz cyclic sequence to its upper and lower complements are inverse of one another.

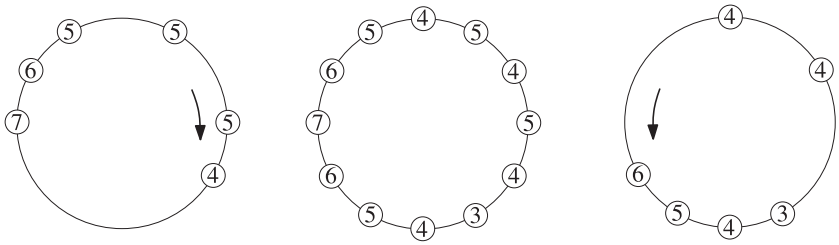

Figure 3. Left: a Łukasiewicz cyclic sequence τ; right: the lower complement $\overline{\tau}^{\downarrow}$; middle: the lower completion of τ (read clockwise) which is also the upper completion of $\overline{\tau}^{\downarrow}$ (read counterclockwise).

2.2. Suitably labeled maps and well-labeled hypermaps: the bijection. First we explain how to construct (the star representation of) a well-labeled hypermap from a suitably labeled map. Let $B \in \mathcal{B}$. Place a black vertex v_f inside each face f of B. Then apply the so-called *BDG rules* (shown in Figure 4 left-part) in f, i.e., when turning around f clockwise, for each *descending* edge e (i.e., at which the label sequence is decreasing), insert a new edge from v_f to the origin of e (note that the vertices of B not incident to any of these new edges are exactly the local min of B). Then erase all the local min of B and all edges of B. Call S the resulting figure.

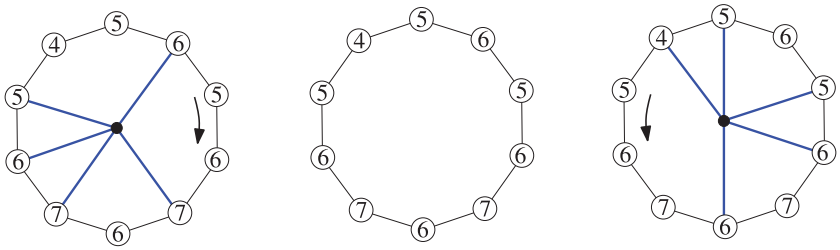

Figure 4. Middle: a face f of a suitably labeled map; left: application of the BDG rules; right: application of the complementary rules. The list of neighbor-labels of the black vertex in counterclockwise order using the complementary rules is the lower complement of the list of neighbor-labels of the black vertex in clockwise order using the BDG rules.

Claim 1. *The resulting figure S is the star-representation of a well-labeled hypermap H.*

The proof is delayed to Section 2.6 (the local condition of being well-labeled is trivially satisfied, the non-trivial part is to show that S is a map, i.e., is connected). Let Φ be the mapping that associates H to B. Figure 5 displays an example of this mapping.

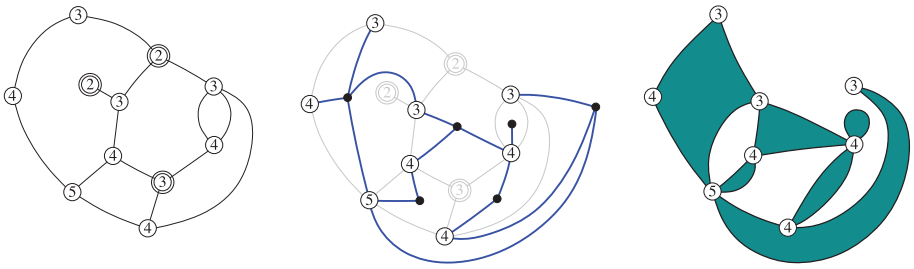

Figure 5. The mapping Φ from a suitably labeled map (local min are surrounded) to a well-labeled hypermap.

We now describe the inverse mapping Ψ (see Figure 6 for an example). Let $H \in \mathcal{H}$. For each light face f of H, denote by $\min(f)$ (resp. $\max(f)$) the minimal (resp. maximal) label of vertices incident to f. Let S be the star representation of H. Consider any face f of S (which identifies to a light face of H). Insert inside f a vertex v_f of label $\min(f) - 1$. Then, for each corner c of f at a labeled (white) vertex v, insert a leg in c. If $\ell(v) > \min(f)$, connect the free extremity of the leg to the next corner of label $\ell(v) - 1$ after c in counterclockwise order around f (note that, when the map is drawn in the plane, going counterclockwise around the outer face amounts to going clockwise around the map). If $\ell(v) = \min(f)$, connect the free extremity of the leg to v_f. Finally delete all black vertices and all edges of S. Denote by B the resulting figure.

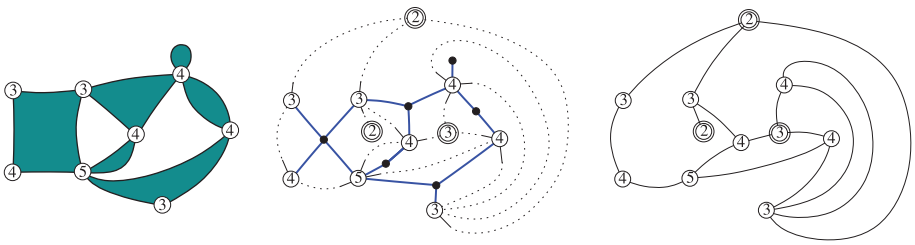

Figure 6. The mapping Ψ from a well-labeled hypermap to a suitably labeled map.

Claim 2. *The resulting figure B is a suitably labeled map.*

The proof is delayed to Section 2.6 (the fact that the labeling is suitable is clear by construction, the nontrivial point is to show that B is a map).

Theorem 1. *The mapping Φ is a bijection between $\mathcal{B}$ and $\mathcal{H}$; the inverse mapping is Ψ. For $B \in \mathcal{B}$ and $H = \Phi(B)$, each vertex v of H corresponds to a non local min vertex v' of B of the same label, and v is a right local max in H if and only if v' is a local max in B, each light face f of H corresponds to a local min vertex of B of label* $\min(f) - 1$, *and each dark face of H of cw-type τ corresponds to a face of B of cw-type $c^{\downarrow}(\tau)$; in particular, the degree of the dark face of H is half the degree of its corresponding face of B.*

The proof that Φ and Ψ are inverse of each other is delayed to Section 2.6. The parameter-correspondence follows rather directly from the way the constructions Φ and Ψ are defined. More precisely, the fact that each face f of H corresponds to a local min of B of label $\min(f) - 1$ follows from the definition of Ψ, and the fact that each dark face of H corresponds to a face of B of cw-type $c^{\downarrow}(\tau)$ follows from the description of Φ (see Figures 3 and 4). Finally, if $v' \in B$ is neither a local min nor a local max, then the corresponding $v \in H$ is not a right local max (see Figure 7(a)), whereas if v is a local max of B, then any right neighbor u of v satisfies $\ell(u) \leq \ell(v)$ (see Figure 7(b)), so that v is a right local max in H.

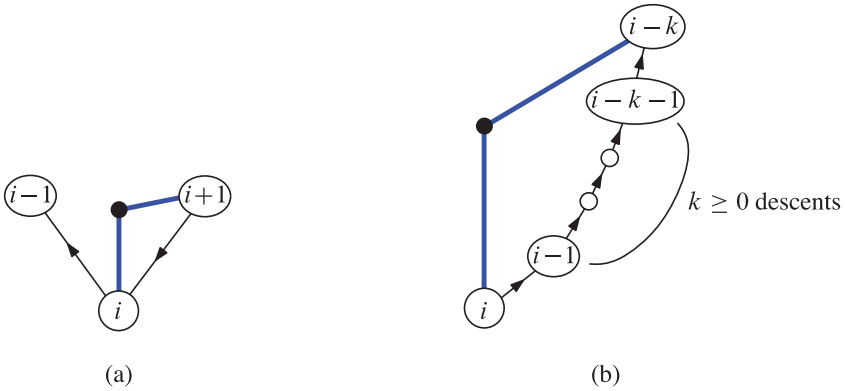

Figure 7. (a) A vertex v of B that is neither a local min nor local max is incident to at least one face of B of the type displayed here, hence has a right neighbor in H of larger label, so that v is not a right local max in H. (b) If a vertex v of B is a local max, then any right neighbor of v in H has smaller (or equal) label, hence v is a right local max in H.

Remark 1. By restricting to the elements of $\mathcal{B}$ whose all faces have degree 4, we recover the bijection of Theorem 1 in [1] between suitably labeled quadrangulations and well-labeled maps (identified to hypermaps by blowing each of their edges into

a dark face of degree 2). Actually, this bijection may also be viewed as equivalent to the Miermont bijection in the planar case: indeed, for a fixed quadrangulation Q, the data of a suitable labeling is equivalent to the data of a set of "sources" and of a "delay vector" in the terminology of [14]. More precisely, taking the local min of the suitable labeling as sources, and their labels as delays, it is not difficult to check that the label of any other vertex is given by the Miermont prescription, namely

$$\ell(v) = \min_{u \text{ local min}} (\mathrm{dist}(u, v) + \ell(u))$$

where dist denotes the graph distance in Q.

2.3. Mirror bijection. We describe here a "mirror" formulation of the bijection Φ. Define a *mirror-well-labeled hypermap* as a vertex-labeled hypermap H such that the "mirror" of H is well-labeled. More precisely, for any edge e with endpoints u, v —with the dark face incident to e on the *left* of e traversed from v to u— we have $\ell(u) \geq \ell(v) - 1$. Denote by $\mathcal{MH}$ the family of mirror-well-labeled hypermaps. The notions of right-neighbor, right local min and right local max are defined in the same way as for the family $\mathcal{H}$ (we do not take a mirror definition). For a dark face f of $H \in \mathcal{MH}$, define the *ccw-type* of f as the cyclic list of labels of the vertices in counterclockwise order around f. Let $B \in \mathcal{B}$. Place a vertex v_f inside each face f of B. Then apply the so-called *complementary rules* (shown in Figure 4 right-part) in f, i.e., when turning around f clockwise, for each *ascending* edge e (i.e., at which the label sequence is increasing), insert a new edge from v_f to the origin of e (note that the vertices of B not incident to any of these new edges are exactly the local max of B). Then erase all the local max of B and all edges of B. Call S the resulting figure, which is a bipartite map, and H the mirror-well-labeled hypermap having S as star-representation. Let Φ^- be the mapping that associates H to B. Let opp be the mapping (operating on any $B \in \mathcal{B}$ or $H \in \mathcal{H}$) that replaces the label of each vertex by its opposite (note that opp maps $\mathcal{B}$ to $\mathcal{B}$ and $\mathcal{H}$ to $\mathcal{MH}$). In fact, given the fact that the complementary rules are the opposite of the BDG rules, we have $\Phi^- = \mathrm{opp} \circ \Phi \circ \mathrm{opp}$. Hence, as a consequence of Theorem 1 we obtain the following result.

Corollary 1. *The mapping Φ^- is a bijection between $\mathcal{B}$ and $\mathcal{MH}$. For $B \in \mathcal{B}$ and $H = \Phi^-(B)$, each vertex v of H corresponds to a non local max vertex v' of B of the same label, and v is a right local min in H if and only if v' is a local min in B, each face f of H corresponds to a local max vertex of B of label* $\max(f) + 1$*, and each dark face of H of ccw-type τ corresponds to a face of B of ccw-type $c^{\uparrow}(\tau)$.*

Remark 2. Upon composing Ψ and Φ^-, we obtain a bijection between $\mathcal{H}$ and $\mathcal{MH}$. Its parameter correspondence, which is left to the reader, is not needed here in all its generality. A relevant specialization will be discussed in Theorem 2.

2.4. Mobiles, vertex-pointed bipartite maps, and vertex-pointed hypermaps. Define a *mobile* as the star-representation of a well-labeled hypermap with a unique light face and with minimal label 1. In other words a mobile is a bipartite plane tree with black unlabeled vertices and white labeled vertices, such that the minimal label is 1 and for any two consecutive neighbors v, u in clockwise order around a black vertex, $\ell(u) \geq \ell(v) - 1$. The following definitions are inherited from the concepts in the associated hypermap with a unique light face. For any black vertex b in a mobile, define the *cw-type* of b as the cyclic sequence given by the labels of the neighbors in clockwise order around b. A white vertex v is called a *right neighbor* of a white vertex u, if u and v are consecutive in counterclockwise order around a black vertex (which is their unique common neighbor). And a white vertex u is called a *right local min* (resp. *right local max*) in the mobile if any right neighbor v of u satisfies $\ell(v) \geq \ell(u)$ (resp. $\ell(v) \leq \ell(u)$).

Claim 3. *Let B be a bipartite map with a pointed vertex v. Then there is a unique suitable labeling of the vertices of B such that v is the unique local min, and $\ell(v) = 0$. This labeling is the* geodesic labeling *with respect to v, i.e., such that $\ell(u)$ is the graph distance* $\mathrm{dist}(v, u)$ *from v to u.*

Proof. It is clear that the geodesic labeling satisfies these properties. Conversely, for any labeling satisfying these properties, each vertex u has a path to v that decreases in label, hence of length $\ell(u)$. So $\ell(u) \geq \mathrm{dist}(v, u)$. Moreover, for any suitable labeling one has trivially $\ell(u) \leq \mathrm{dist}(v, u)$ (the sequence of labels along a geodesic path from v to u increases by at most 1 at each edge). Hence $\ell(u) = \mathrm{dist}(v, u)$ for any vertex u. □

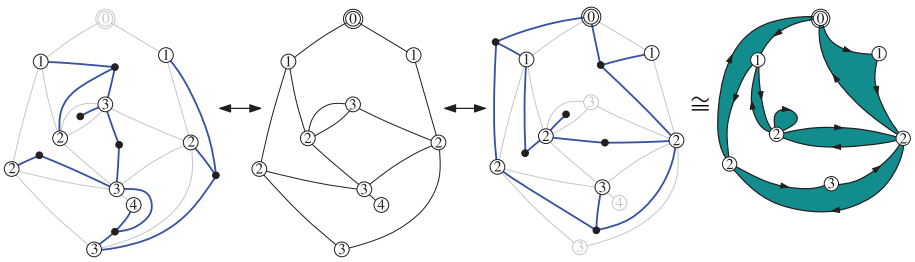

Figure 8. A vertex-pointed map endowed with its geodesic labeling, on its left the associated mobile, on its right the associated vertex-pointed hypermap (endowed with its geodesic labeling).

Applying Theorem 1 to the subfamily of $\mathcal{B}$ with a unique local min vertex v and with $\ell(v) = 0$, we recover the following result from [7] (see the left part of Figure 8 for an illustration).

Proposition 1. *The mapping Φ specializes to a bijection between vertex-pointed bipartite maps and mobiles with the following properties. For B a vertex-pointed bipartite map, endowed with its geodesic labeling, and M the corresponding mobile, each white vertex v of M corresponds to a non-pointed vertex v' of B of the same label, and v is a right local max of M if and only if v' is a local max of B. And each black vertex of M of cw-type τ corresponds to a face of B of cw-type $c^{\downarrow}(\tau)$.*

Given a hypermap H, define the *canonical orientation* of H as the orientation where each edge is directed so as to have its incident dark face on its right. If H has a pointed vertex v, the *geodesic labeling* of H with respect to v is the labeling of vertices where $\ell(u)$ gives the length of a shortest directed path (in the canonical orientation) from v to u. Similarly as in Claim 3 (and with the same proof arguments) we have the following claim.

Claim 4. *Let H be a hypermap with a pointed vertex v. Then there is a unique mirror-well-labeling of the vertices of H such that v is the unique right local min, and $\ell(v) = 0$. This labeling is the geodesic labeling with respect to v.*

Applying Corollary 1 to the subfamily of $\mathcal{MH}$ with a unique local min vertex v and with $\ell(v) = 0$, we obtain the following result (see the right part of Figure 8 for an illustration) see the following proposition.

Proposition 2. *The mapping Φ^{-} specializes to a bijection between vertex-pointed bipartite maps and vertex-pointed hypermaps with the following properties. For B a vertex-pointed bipartite map endowed with its geodesic labeling, and H the corresponding vertex-pointed hypermap endowed with its geodesic labeling, each light face f of H corresponds to a local max vertex of B of label $\max(f) - 1$, each vertex of H corresponds to a non local max vertex of B of the same label (so the pointed vertices correspond to each other), and each dark face of H of ccw-type τ corresponds to a face of B of ccw-type $c^{\uparrow}(\tau)$.*

As shown in Figure 9 (right part), in the case where all dark faces of the hypermap have degree 2, we recover the bijection of Ambjørn and Budd between vertex-pointed maps and vertex-pointed quadrangulations.

Remark 3. There is already a classical bijection between (vertex-bicolored) bipartite maps and hypermaps such that each face of degree $2s$ in the bipartite map corresponds to a dark face of degree s in the corresponding hypermap, see Figure 10 (note that the bijection of Figure 10 is the application of Φ with the special suitable labeling where every vertex at even distance from the pointed vertex has label 1 and every vertex at odd distance has label 0). However, this bijection does not have the distance conservation property of Proposition 2.

Composing the bijections of Propositions 1 and 2 we obtain Theorem 2 (see Figure 8).

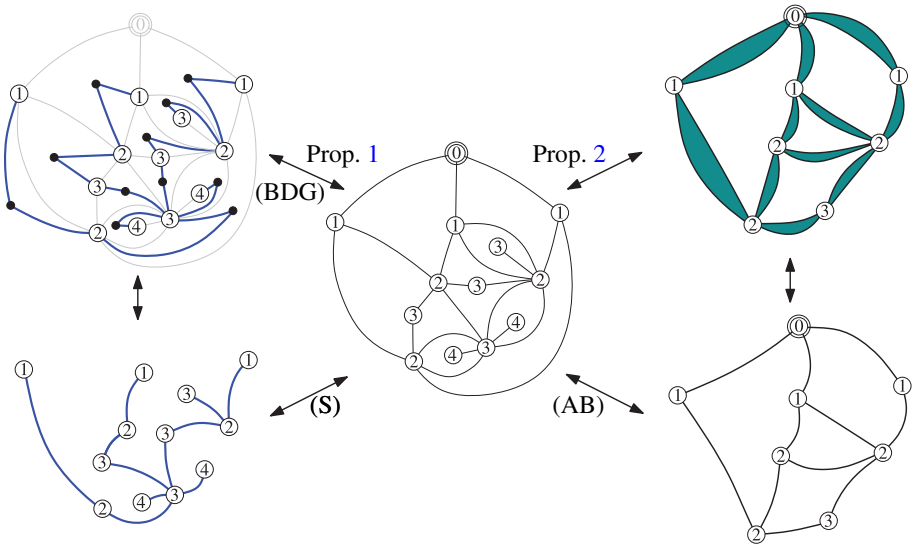

Figure 9. In the case where the intermediate suitably labeled map is a vertex-pointed quadrangulation, the mobile obtained by the BDG rules (bijection in [7], recovered in Proposition 1) simplifies to a well-labeled tree (with minimal label 1), which corresponds to Schaeffer's bijection [10], [16] (symbol S in the diagram). Moreover, the vertex-pointed hypermap obtained by the complementary rules (Proposition 2) simplifies to a vertex-pointed map, which corresponds to the bijection of Ambjørn and Budd [1] (symbol AB in the diagram) between vertex-pointed quadrangulations and vertex-pointed maps.

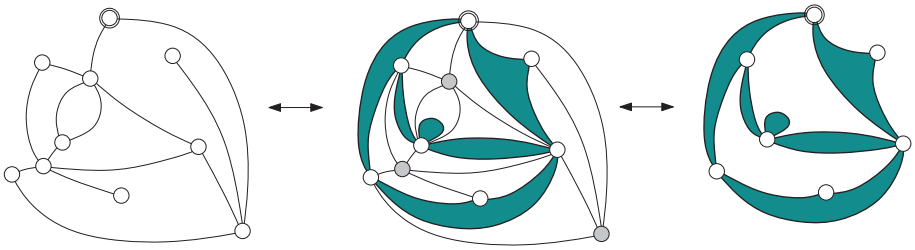

Figure 10. The usual bijection between vertex-pointed bipartite maps and vertex-pointed hypermaps. From left to right: color white (resp. gray) the vertices that are at even (resp. odd) distance from the pointed vertex, then inside each face f of the bipartite map insert a dark face that connects the white corners of f. From right to left: insert a gray vertex v_f inside each light face f of the hypermap, and connect v_f to all corners around f.

Theorem 2. *The mapping* $\Phi \circ (\Phi^-)^{-1}$ *specializes to a bijection between vertex-pointed hypermaps and mobiles with the following properties. For* H *a vertex-pointed hypermap endowed with its geodesic labeling, and* M *the corresponding mobile, each light face* f *of* H *corresponds to a right local max of* M *of label* $\max(f)+1$*, each unpointed vertex of* H *corresponds to a non right local max vertex of* M *of the same label and each dark face of* H *of ccw-type* τ *corresponds to a black vertex of* M *of cw-type* $\overline{\tau}^{\uparrow}$.

In particular, for $p \geq 2$, $\Phi \circ (\Phi^-)^{-1}$ *restricts to a bijection between vertex-pointed* p-hypermaps (*hypermaps with all dark faces of degree* p) *and* p-mobiles (*mobile with all black vertices of degree* p).

Note that there is already a bijection in [7] between vertex-pointed hypermaps and certain labeled decorated (multitype) plane trees. The bijection of [7] (which also relies on the geodesic labeling of the vertex-pointed hypermap) has the advantage that it keeps track of the degrees of light faces, an information that is lost with the bijection of Theorem 2. However the price to pay is that the decorated trees in [7] are far more complicated than the mobiles of Theorem 2.

2.5. Specialization to constellations. For $p \geq 2$, a (*planar*) *p-constellation* is a p-hypermap (as defined in Theorem 2) with all light faces of degree a multiple of p. Constellations are also characterized as p-hypermaps that can be vertex-colored, with colors $0, 1, \ldots, p-1$, such that in clockwise order around any dark face the colors are $0, 1, \ldots, p-1$ (seen this way they correspond to certain factorizations, into p factors, in the symmetric group). Equivalently, given a vertex-pointed p-hypermap H endowed with its geodesic labeling, H is a p-constellation if and only if the labels modulo p of the vertices in clockwise order around each dark face are $0, 1 \ldots, p-1$. A Łukasiewicz cyclic sequence of length r is said to be *descending* if it has a unique rise and $r-1$ descents (by 1). Define a *p-descending mobile* as a p-mobile with all black vertices of descending cw-type. From the discussion above, a p-hypermap H, endowed with its geodesic labeling, is a p-constellation if and only if all its dark faces are of descending ccw-type. Hence, as a specialization of Theorem 2 we obtain:

Proposition 3. *The mapping* $\Phi \circ (\Phi^-)^{-1}$ *specializes to a bijection between vertex-pointed p-constellations and p-descending mobiles, with the same correspondence of parameters as in Theorem 2.*

Remark 4. Using the trivial identification of 2-constellations with bipartite maps, we may combine Proposition 3 and Proposition 2, to obtain a bijection between 2-descending mobiles and vertex-pointed hypermaps. In this bijection, black vertices and right local max of a mobile correspond respectively to edges and dark faces of the associated hypermap.

The bijection between vertex-pointed p-constellations and p-descending mobiles is shown in Figure 11 for $p = 3$ (forgetting the bottom-left drawing for the moment)

and in Figure 12 for $p = 2$ (constellations identify to bipartite maps by shrinking each dark face of degree 2 into an edge and 2-descending mobiles identify to suitably labeled plane trees – with minimum label 1 – by erasing the black vertices).

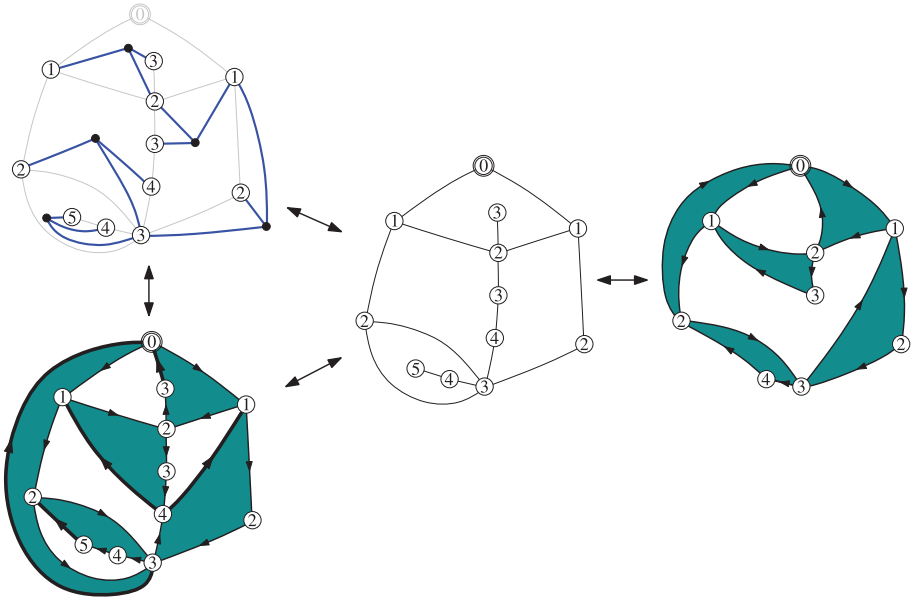

Figure 11. Middle: a vertex-pointed stretched 6-angulation. Right: the associated (by the complementary rules) vertex-pointed 3-constellation. Top-left: the associated (by the BDG rules) mobile. Bottom-left: the 4-regular constellation obtained by drawing a diagonal in each (stretched) face from the largest to the smallest vertex. Upon composing these elementary bijections, we obtain Proposition 3 (connecting top-left to right) and Proposition 4 (connecting bottom-left to right).

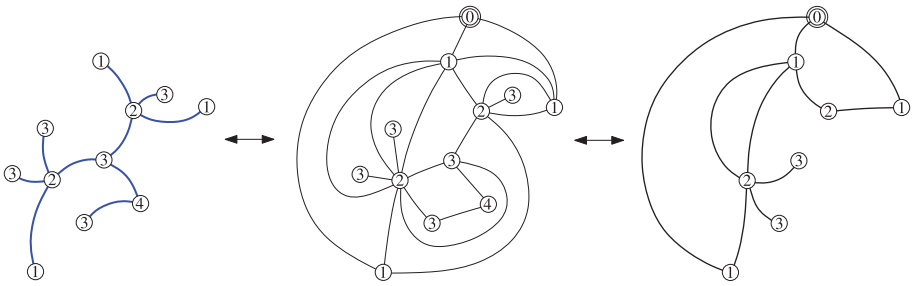

Figure 12. In the case $p = 2$, a p-constellation identifies to a bipartite map G (on the right side), and a p-descending mobile identifies to a suitably labeled plane tree T with minimal label 1 (left side). Each face of G corresponds to a local max of T, each unpointed vertex of G corresponds to a non local max vertex of T of the same label, and each edge of G of type $(i, i-1)$ corresponds to an edge of T of type $(i+1, i)$. The bijection is a specialization of the bijection of Ambjørn and Budd using stretched vertex-pointed quadrangulations as intermediate objects (middle).

Let B be a vertex-pointed bipartite map endowed with its geodesic labeling. A face f of B, of even degree $2s$, is said to be *stretched* if its type (cw or ccw) is of the form $i, i+1, \ldots, i+s-1, i+s, i+s-1, \ldots, i+1$, i.e., there are s rises followed by s descents. And B is called *stretched* if all its faces are stretched. Stretched vertex-pointed $2p$-angulations are the bijective intermediates in Proposition 3 (i.e., these are the maps in correspondence with p-descending mobiles via Φ and with vertex-pointed p-constellations via Φ^-). Moreover, as shown in [7], p-descending mobiles are in bijection with vertex-pointed $(p+1)$-constellations with all light faces of degree $p+1$ (shortly called $(p+1)$-regular constellations – note that those are nothing but Eulerian $(p+1)$-angulations endowed with a proper bi-coloring of their faces). We provide here a simple shortcut (to jump over p-descending mobiles) in the bijective chain

vertex-pointed p-constellations

$\longleftrightarrow$ vertex-pointed stretched $2p$-angulations

$\longleftrightarrow$ p-descending mobiles

$\longleftrightarrow$ vertex-pointed $(p+1)$-regular constellations.

Given a vertex-pointed stretched $2p$-angulation B, draw in each (stretched) face a diagonal e from the largest to the smallest vertex. This splits the face into two faces of degrees $p+1$, and we color the one on the right of e as dark and the one on the left of e as light. The resulting figure is clearly a vertex-pointed $(p+1)$-regular constellation E. In addition, if B is endowed with its geodesic labeling, then the induced labeling on E is exactly the geodesic labeling of E. The inverse mapping is easy. Given a $(p+1)$-regular constellation E, endow E with its geodesic labeling, which has the property that the labels in clockwise (resp. counterclockwise) order around each dark (resp. light) face are of the form $i, i+1, \ldots, i+p$. Erasing the edges of the form $i, i+p$, we naturally obtain a stretched (vertex-pointed) bipartite $2p$-angulation endowed with its geodesic labeling. To summarize, we obtain the following result.

Proposition 4. *There is a bijection between vertex-pointed p-constellations and vertex-pointed $(p+1)$-regular constellations with the following properties. For C a vertex-pointed p-constellation and E the corresponding vertex-pointed $(p+1)$-regular constellation (both endowed with their geodesic labeling), each face f of C corresponds to a right local max vertex of E of label $\max(f)+1$, and each vertex v of C corresponds to a non right local max vertex v' of E of the same label.*

There is already a classical bijection between vertex-pointed p-constellations and vertex-pointed $(p+1)$-regular constellations, using the characterization in terms of vertex-coloring, see Figure 13. However, similarly as in Proposition 2, the bijection of Proposition 4 has the advantage that it preserves the distance to the pointed vertex.

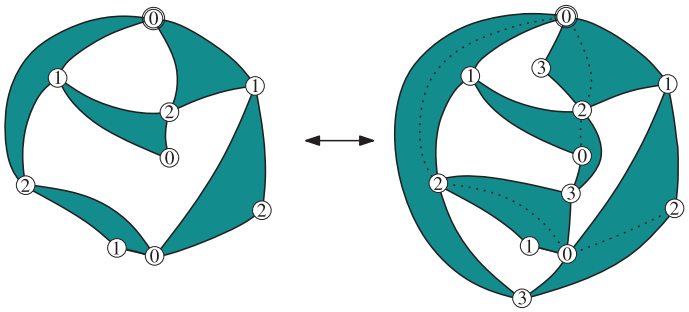

Figure 13. The usual bijection between vertex-pointed p-constellations and vertex-pointed $(p+1)$-regular constellations. From left to right: add a vertex of color p in each light face and extend each dark face by making its edge $(p-1,0)$ pass by the vertex in the light face to its left. From right to left: draw a diagonal in each dark face between the vertices of color 0 and $p-1$, then erase the vertices of color p and their incident edges.

2.6. Proof that the mappings Φ/Ψ give a bijection

2.6.1. Proof of Claim 1. Let S be the figure obtained from $B \in \mathcal{B}$ by applying the BDG rules, and then deleting the local min and the edges of B. We show here that S is a map, i.e., is connected. A first easy remark is that S has no isolated vertices, i.e., each vertex of S has at least one incident edge in S. Let s_v, s_e, s_f be the numbers of vertices, edges, and faces[1] of S. Let m be the number of local min of B. By the BDG rules, s_e is the number of edges of B, and $s_v + m$ is the number of vertices plus the number of faces of B. Hence, by the Euler relation applied to B, $s_v + m = s_e + 2$. Moreover, the Euler relation applied to S ensures that $s_v + s_f = s_e + 1 + k$, where k is the number of connected components of S. Hence, S is connected if and only if $s_f \leq m$ (indeed, S is connected if and only if $k \leq 1$). To prove that $s_f \leq m$, it is enough to show that (seeing S and B as superimposed) there is at least one local min of B inside each face f of S. Let w be a white vertex of smallest label on the boundary of f. Since S has no isolated vertices, it is easy to see that there is an edge e incident to w on the boundary of f and such that the corner following e in counterclockwise order around w is in f. By the BDG rule shown in Figure 4 left, the next edge after e in counterclockwise order around w is an edge e' of B that leads to a white vertex w' of label $\ell(w) - 1$. By the choice of e, e' is inside f, and by minimality of $\ell(w)$, w' can not be on the boundary of f. Since w' is in f but not on its boundary, w' does not belong to S, hence w' is a local min of B. Hence there is a local min of B inside f.

[1] A face of a (not necessarily connected) graph G embedded on a surface Σ is defined as a connected component of $\Sigma \backslash G$. Note that the boundary of a face might have several components if G is not connected or if Σ has nonzero genus.

2.6.2. Proof of Claim 2 and that $\Phi \circ \Psi = \mathrm{Id}$. Let $H \in \mathcal{H}$, let S be the star representation of H, and superimpose S with $B := \Psi(H)$. Looking at Figure 14(b) it is clear that any pair of connected white vertices of S are connected in B. Since S is connected, B is also connected, i.e., is a map.[2] In addition, it is clear also from the figure that the edges of S will exactly be those selected by the BDG rules. Hence $\Phi(B) = H$.

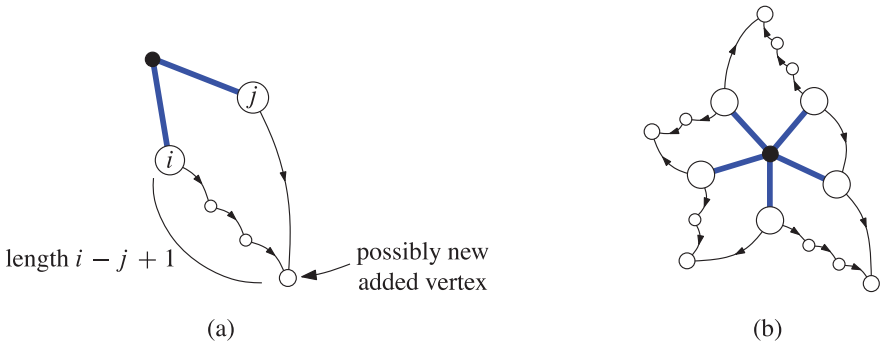

Figure 14. (a) Situation (after applying Ψ) for a corner at a black vertex of S (edges of B are oriented in label decreasing direction). (b) Situation (after applying Ψ) around a black vertex of S: each black vertex of S yields a face of B.

2.6.3. Proof that $\Psi \circ \Phi = \mathrm{Id}$. Let $B \in \mathcal{B}$, $H = \Phi(B)$, and S the star-representation of H. In the following it is convenient to see B as superimposed with S. An easy observation (following from the BDG rules) is that, if we direct the edges of B in label-decreasing way, then each corner c of S at a white vertex v —since B and S are superimposed, there is a bunch of edges of B in c— contains a unique edge of B going out of v, which is the clockwise-most in c (note that this local property is to be satisfied after applying Ψ), see Figure 15(a). Denote by e_c this edge. We have seen in Section 2.6.1 that $H \in \mathcal{H}$, there is exactly one local min of B strictly inside each face f of S, and this local min has label $\min(f) - 1$. So the first step of Ψ (adding a vertex inside each face f of label $\min(f) - 1$) is the inverse of the last step of Φ (deleting all the local min); and in addition for each corner c of S at a white vertex v, if e_c goes to the local min in the face incident to c, then e_c will be created by Ψ. It remains to show that for each corner c such that e_c does not go to a local min (otherly stated, for each edge e of B not incident to a local min), e_c will be created by Ψ. Let f be any face of S, with v_f the local min of B inside f, and let e be an edge of B inside f and not incident to v_f. Adding e to f splits f into two faces $L_f(e)$, $R_f(e)$ respectively on the left and on the right of e directed in label decreasing way. Let u be

[2] Since the arguments are to be extended to higher genus in Section 2.7 it is good to also have a polygon-gluing proof that $\boldsymbol{B}$ is a map: as can be seen from Figure 14(b), each black vertex b of $\boldsymbol{S}$ yields a face f_b of $\boldsymbol{B}$, and it is easy to see (since each face of $\boldsymbol{S}$ is covered by sectors of the form of Figure 14(a)) that these faces f_b cover the entire surface (a sphere up to now).

the extremity of e of largest label and v the extremity with smaller label, say $\ell(u) = i$ and $\ell(v) = i - 1$. To show that e will be created when applying Ψ (to S), it remains to establish the following property.

Claim 5. *The local min v_f is inside $L_e(f)$, v has a unique incident corner in $R_e(f)$ (the one delimited by e on the right side) and any other corner in $R_e(f)$ at a white labeled vertex w satisfies $\ell(w) \geq i$.*

Proof of the claim. Recall the BDG rule (illustrated in Figure 15): for each edge e of S, with black extremity b and white (labeled) extremity w, the next edge after e in counterclockwise order around w leads to a white vertex of label $\ell(w) - 1$. Let w_ℓ be a white vertex of smallest possible label on the contour of $L_e(f)$, note that $w_\ell \neq u$. Since $w_\ell \neq u$, the BDG rule recalled above implies that w_ℓ has a neighbor of label $\ell(w_\ell) - 1$ in $L_e(f)$, either at v_f or on the contour of $L_e(f)$. The second case is excluded by minimality of w_ℓ, so we conclude that v_f is inside $L_e(f)$, see Figure 15(b). The statement about $R_e(f)$ is proved similarly. Denote by c the corner of $R_e(f)$ that is incident to v and delimited by e on the right side. Call a corner of $R_e(f)$ admissible if it is different from c and incident to a white vertex. Choose an admissible corner c_0 in $R_e(f)$ of smallest possible label (label of the incident white vertex). Let w_0 be the white vertex incident to c_0. Again, since $c_0 \neq c$ the BDG rule implies that w_0 has a neighbor of label $\ell(w_0) - 1$ on the contour of $R_e(f)$. This neighbor is necessarily v (otherwise it would yield an admissible corner of smaller label than c_0, contradicting the minimality of c_0), hence $\ell(w_0) = i$. □

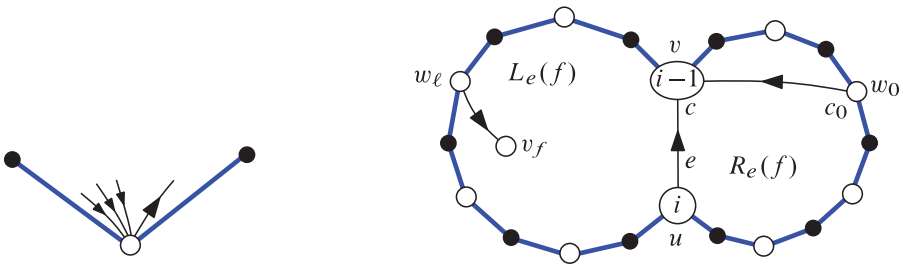

Figure 15. (a) After applying Φ to B, each corner c of S contains a unique edge of B going out, which is the clockwise-most edge of B inside c. (b) Situation in the proof of Claim 5. The shown edges of B are directed in the label-decreasing way.

2.7. Extension to higher genus. Up to now the bijective results have been stated and proved with maps and hypermaps on the sphere, but everything can be defined, stated and proved in the same way in genus $g \geq 0$ (the sphere corresponds to $g = 0$, recall that a map of genus g is a connected graph G embedded on the genus g surface

Σ such that any component of $\Sigma \backslash G$ is a topological disk). We point out here the few places where one can not copy verbatim.

In the proofs, the only place involving g as a parameter is in the use of the Euler relation in the proof of Claim 1. In genus g, the Euler relation applied to B gives $s_v + m = s_e + 2 - 2g$, and the Euler relation applied to S ensures that $s_v + s_f \geq s_e + 2 - 2g$, with equality if and only if S is a map of genus g. Hence S is a map of genus g if and only if $s_f \leq m$, as in the genus 0 case.

In the definitions, note that a mobile (i.e., the star-representation of a well-labeled hypermap with a unique light face and minimal label 1) is not a tree in higher genus but a unicellular map of genus g. And the notion of constellation in genus g has to be defined in terms of the color-property (in higher genus, the condition of light face-degrees being multiple of p is strictly weaker than the condition with colors), that is, for $p \geq 2$, a *p-constellation* in genus g is a p-hypermap of genus g whose vertices can be colored, with colors in $0, 1, \ldots, p-1$, such that the colors of vertices in clockwise order around any dark face are $0, 1, \ldots, p-1$. The extension of Proposition 1 (bijection between vertex-pointed bipartite maps and mobiles) to higher genus was first given in [9].

3. Two-point functions depending on a single size parameter

In this section we shall use specializations of the above bijections to compute distance-dependent two-point functions for a number of families of maps or hypermaps. More precisely, we shall concentrate on 2-hypermaps, i.e., hypermaps having all their dark faces of degree 2, and 3-*hypermaps* with all their dark faces of degree 3. Recall that *general maps*, whose two-point function was already obtained in [1], are trivially identified with 2-hypermaps by blowing each edge of the map into a dark face of degree 2. We shall also consider the case of 2-constellations, trivially identified with *bipartite maps*, and that of 3-*constellations*. All these maps will be counted according to their natural size parameter, namely the number of edges (for maps) or dark faces (for hypermaps).

The (distance-dependent) *two-point function* of a class of maps is, informally speaking, the generating function of such maps with two marked points at a prescribed distance. More precisely, we consider planar (hyper)maps that are both vertex-pointed and rooted, i.e., with a marked oriented edge (the *root edge*). In the case of hypermaps, we furthermore assume that the root edge is oriented in such a way that its incident dark face (the *root face*) lies on its right. The two-point function is defined as the generating function of these vertex-pointed and rooted (hyper)maps with prescribed geodesic distances from the pointed vertex to all vertices incident to the root edge (for maps) or to the root face (for hypermaps). Since we consider only a single size parameter, the two-point function depends on a single formal variable t, the weight per edge or dark face.

The reader shall be warned that, in order to avoid introducing too many symbols, indexes or subscripts, we will keep the same notation for the two-point function and related quantities regardless of the class of maps considered.

3.1. The two-point function of general maps. Consider a pointed rooted map (i.e., a map with a pointed vertex and a marked oriented edge): we say that its root edge is of type (k, j) if its origin and endpoint are at respective distances k and j from the pointed vertex. Here k and j are non-negative integers satisfying $|j - k| \leq 1$. Following the notation of [8], we denote by $R_i \equiv R_i(t)$, $i \geq 1$, the generating function of pointed rooted maps *enumerated with a weight t per edge* whose root edge is of type $(j-1, j)$ for $j \leq i$. By reversing the orientation of the root edge, pointed rooted maps whose root edge is of type $(j+1, j)$ for $j \leq i$ are enumerated by R_{i+1}. We finally denote by $S_i^2 \equiv S_i(t)^2$, $i \geq 0$, the generating function of pointed rooted maps whose root edge is of type (j, j) for $j \leq i$ (we write this generating function as a square to stick to the notation of [8]). Note that the generating function of pointed rooted maps where the endpoint of the root edge is at distance at most i from the origin is equal to $R_i + R_{i+1} + S_i^2$.

3.1.1. Computation from the bijective approach. Using the trivial identification of maps with 2-hypermaps, R_i may alternatively be understood as the generating function for vertex-pointed and rooted 2-hypermaps, with a weight t per dark face, and a root face of ccw-type $\tau = (j, j-1)$ for $j \leq i$ if we endow the hypermap with its geodesic labeling. From Theorem 2, those are in one-to-one correspondence with 2-mobiles, i.e., mobiles having all their black vertices of degree 2, with a marked black vertex (in correspondence with the root face) of cw-type $\overline{\tau}^{\uparrow} = (j, j+1)$, $j \leq i$.

Similarly, S_i^2 may be viewed as the generating function for vertex-pointed and rooted 2-hypermaps, with a weight t per dark face, and a root face of ccw-type $\tau = (j, j)$ for $j \leq i$ (under the geodesic labeling), one side of the root face being distinguished (in correspondence with the root edge). From Theorem 2, those are now in in one-to-one correspondence with 2-mobiles with a marked black vertex of cw-type $\overline{\tau}^{\uparrow} = (j+1, j+1)$, $j \leq i$, one of the incident half edges being distinguished.

Recall that mobiles are required to have a minimal label 1. The summation over all $j \leq i$ allows however to waive this constraint. Indeed, shifting the labels by $i - j \geq 0$ in a mobile with a marked black vertex of cw-type $\overline{\tau}^{\uparrow} = (j, j+1)$ (resp. $\overline{\tau}^{\uparrow} = (j+1, j+1)$) produces a new labeled tree with marked black vertex of cw-type $\overline{\tau}^{\uparrow} = (i, i+1)$ (resp. $\overline{\tau}^{\uparrow} = (i+1, i+1)$) whose minimal label $1 + i - j$ is now, after summation over j, an arbitrary integer between 1 and i (respectively $i+1$). We shall call *floating* mobiles these new objects with an arbitrary positive minimal label (the rules for labels around a black vertex remain unchanged).

Denoting by $T_i = T_i(t)$ the generating function of floating 2-mobiles planted at a white vertex labeled i, enumerated with a weight t per black vertex, we deduce

immediately the identifications

$$R_i = 1 + tT_iT_{i+1}, \quad i \geq 1, \tag{1a}$$

and

$$S_i = \sqrt{t}T_{i+1}, \qquad i \geq 0, \tag{1b}$$

where we incorporated in R_i a conventional term 1. Now we have at our disposal explicit expressions for the generating function T_i, as obtained for instance by solving the equation

$$T_i = \frac{1}{1 - t(T_{i-1} + T_i + T_{i+1})}, \quad i \geq 1 \tag{2}$$

with initial condition $T_0 = 0$ (this equation simply expresses the recursive nature of planted floating 2-mobiles, namely that a floating 2-mobile planted at a white vertex labeled i may be viewed as a sequence of planted floating 2-mobiles – attached to the root vertex via bivalent black vertices – having themselves a root label $i-1$, i or $i+1$). From various techniques, it was found (see [5]) that

$$T_i = T\frac{(1-y^i)(1-y^{i+3})}{(1-y^{i+1})(1-y^{i+2})} \quad \text{where } T = 1 + 3tT^2 \text{ and } y + \frac{1}{y} + 1 = \frac{1}{tT^2}. \tag{3}$$

Here, and for similar equations below, we always pick for T the solution satisfying $T = 1 + O(t)$ and for y the solution with modulus less than 1. Plugging this formula in the expressions for R_i and S_i above, we deduce, after simplification, that

$$R_i = R\frac{(1-y^{i+1})(1-y^{i+3})}{(1-y^{i+2})^2} \quad \text{where } R = 1 + tT^2 \tag{4}$$

and

$$\begin{aligned} S_i &= S\frac{(1-y^{i+1})(1-y^{i+4})}{(1-y^{i+2})(1-y^{i+3})} \\ &= S - \sqrt{Ry}\Big(\frac{1-y^{i+2}}{1-y^{i+3}} - \frac{1-y^{i+1}}{1-y^{i+2}}\Big), \quad \text{where } S = \sqrt{t}T. \end{aligned} \tag{5}$$

Note that $R = \lim_{i\to\infty} R_i$ and $S^2 = \lim_{i\to\infty} S_i^2$ may be understood as the generating functions for pointed rooted maps whose root edge is of type $(j-1, j)$ and (j, j) respectively *without bound on* j. In particular, the generating function for pointed rooted planar maps is $2(R-1) + S^2 = 3tT^2 = T - 1$ which (from the Schaeffer bijection for instance) is known to be half the generating function for pointed rooted quadrangulations. This result could have been deduced directly from the "trivial" bijection between general maps and quadrangulations.

Let us finally compute the generating function V_i for vertex-pointed maps, enumerated with a weight t per edge, with an extra marked vertex at distance $j \leq i$ from the pointed vertex, with $i \geq 1$. Recall that such doubly-pointed maps (supposedly drawn on the sphere) may present a k-fold symmetry by rotation around their two marked vertices (supposedly drawn at antipodal positions). As customary, we decide to enumerate maps with this k-fold symmetry with a *symmetry factor* $1/k$. Only with this definition has V_i a simple expression. As before, V_i may alternatively be understood as the generating function (with symmetry factors) for vertex-pointed 2-hypermaps with an extra marked vertex labeled $j \leq i$ under the geodesic labeling. From Theorem 2, these are in one-to-one correspondence with 2-mobiles with a marked non-right-local-max vertex of the same label j. Shifting the labels by $(i-j)$ and summing over all $j \leq i$, V_i is the generating function for floating 2-mobiles with a marked non-right-local-max vertex labeled i. Upon decomposing such a mobile at the marked vertex, we obtain a cyclic sequence of planted subtrees, at least one of them having root label $i+1$, which translates into the expression

$$\begin{aligned} V_i &= \sum_{k\geq 1} \frac{t(t(T_{i-1}+T_i+T_{i+1}))^k}{k} - \sum_{k\geq 1} \frac{(t(T_{i-1}+T_i))^k}{k} \\ &= \log\Big(\frac{1-t(T_{i-1}+T_i)}{1-t(T_{i-1}+T_i+T_{i+1})}\Big) \\ &= \log(T_i(1-t(T_{i-1}+T_i))) \\ &= \log(1+tT_iT_{i+1}) \\ &= \log(R_i), \end{aligned}$$

valid for $i \geq 1$ (the $1/k$ factors on the first line come from the fact that sequences of subtrees differing by a cyclic shift must be identified).

3.1.2. Comparison with the continued fraction approach. It is interesting to compare the explicit expressions (4) and (5) to those obtained from the continued fraction approach developed in [8] for maps with a control of their face degrees. Note that enumerating maps with a weight t per edge is equivalent to enumerating maps *with unbounded face degrees* and a weight $g_k = t^{k/2}$ per face of degree k. The continued fraction approach allows to write

$$R_i = R\frac{u_iu_{i+2}}{u_{i+1}^2} \tag{6a}$$

and

$$S_i = S - \sqrt{R}\Big(\frac{\tilde{u}_{i+2}}{u_{i+2}} - \frac{\tilde{u}_{i+1}}{u_{i+1}}\Big) \tag{6b}$$

where R and S^2 have the same interpretation as above as pointed rooted map generating functions and where u_i and $\tilde{u}_i$ may be expressed in terms of $(i+1)\times(i+1)$

Hankel determinants H_i and $\tilde{H}_i$ (with the notation of [8], $u_i = H_{i-2}/R^{(i-1)(i-2)/2}$ and $(i-1)Su_i - \sqrt{R}\tilde{u}_i = \tilde{H}_{i-2}/R^{(i-1)(i-2)/2}$). R and S are determined by the system (see equation (1.6) in [8])

$$S = \sum_{k=1}^{\infty} t^{k/2} P(k-1, R, S), \tag{7a}$$

$$R = 1 + \frac{1}{2}\sum_{k=1}^{\infty} t^{k/2} P(k, R, S) - \frac{S^2}{2}, \tag{7b}$$

where $P(k, R, S)$ denotes the generating function of three-step paths, i.e., lattice paths in the discrete Cartesian plane consisting of up-steps $(1, 1)$, level-steps $(1, 0)$ and down-steps $(1, -1)$, starting at $(0, 0)$ and ending at $(k, 0)$, with a weight S attached to each level-step and a weight $\sqrt{R}$ attached to each up- or down-step. The summation over three-step paths yields immediately

$$S = \sqrt{t}(1 - 2\sqrt{t}S + t(S^2 - 4R))^{-1/2},$$

$$R = 1 + \frac{1}{2}\Big(\frac{S}{\sqrt{t}} - 1\Big) - \frac{S^2}{2},$$

from which we deduce the explicit values

$$S = \frac{1 - \sqrt{1 - 12t}}{6\sqrt{t}},$$

$$R = \frac{1 + 12t - \sqrt{1 - 12t}}{18t}.$$

It is readily seen that these values coincide with the above expressions $S = \sqrt{t}T$ and $R = 1 + tT^2$ for a function T given by

$$T = \frac{1 - \sqrt{1 - 12t}}{6t}$$

which is precisely the solution of $T = 1 + 3tT^2$. This corroborates, as it should, our results for R and S.

As for u_i and $\tilde{u}_i$, it is known that, in the case of maps with bounded face degrees, the related Hankel determinants may be expressed as symplectic Schur functions whose variables are the solutions x of a *characteristic equation*; see equation (1.10) in [8] (up to a $x \to 1/x$ symmetry, this equation admits as many solutions as the maximal allowed face degree minus 2). As such, u_i and $\tilde{u}_i$ may be expressed in terms of determinants of a fixed size, independent of i. For unbounded face degrees however, we have no such simplification *a priori* and in the present case, we have not

been able to derive simple expressions for u_i and $\tilde{u}_i$ directly from their expressions via Hankel determinants. Still it is instructive to write the characteristic equation

$$1 = \sum_{k=2}^{\infty} t^{k/2} \sum_{q=0}^{k-2} P(k-2-q, R, S)\Big(\sqrt{R}x + S + \frac{\sqrt{R}}{x}\Big)^q.$$

By exchanging the sums, it may be rewritten as

$$1 = \frac{t(1-2\sqrt{t}S + t(S^2-4R))^{-1/2}}{1-\sqrt{t}\Big(\sqrt{R}x + S + \dfrac{\sqrt{R}}{x}\Big)}$$

which, upon setting $S = \sqrt{t}T$ and $R = 1+tT^2$, and using $T = 1+3tT^2$, simplifies into

$$x^2 + \frac{1}{x^2} + 1 = \frac{1}{tT^2}.$$

Note that, up to obvious symmetries $x \to -x$ and $x \to 1/x$, this equation determines a unique solution. Moreover, comparing with our bijective results, we are led to the identification $x^2 = y$, while eqs. (4) and (5) show that $u_i = c\lambda^i(1-x^{2i+2})$ for some (undetermined) c and λ and $\tilde{u}_i = c\lambda^i x(1-x^{2i})$. It is remarkable that u_i and $\tilde{u}_i$ admit such a simple form: this property still awaits a proper explanation in the continued fraction approach.

3.1.3. Applications. As a simple application of the above formulas, we may compute the average number of edges of type $(i-1,i)$, (i,i) or $(i+1,i)$ in an infinitely large vertex-pointed map, i.e., a vertex-pointed map with n edges in the limit $n \to \infty$. (Note that, in all rigor, our computation incorporates a symmetry factor $1/k$ to those vertex-pointed maps having a k-fold symmetry. These symmetric maps are however negligible in the large n limit.) The large n asymptotics is easily captured by the singularity of the above generating functions when $t \to 1/12$. We have singularities of the form

$$R_i|_{\text{sing.}} \sim (1-12t)^{3/2}\delta_i,$$

$$S_i^2|_{\text{sing.}} \sim (1-12t)^{3/2}\eta_i,$$

with values of δ_i and η_i easily computed from the exact expressions above for R_i and S_i. We immediately deduce the large n asymptotics $[t^n]R_i \sim \frac{12^n}{\sqrt{\pi}n^{5/2}}\frac{3}{4}\delta_i$ and $[t^n]S_i^2 \sim \frac{12^n}{\sqrt{\pi}n^{5/2}}\frac{3}{4}\eta_i$, to be compared with the asymptotics $\frac{12^n}{2\sqrt{\pi}n^{5/2}}$ for the number of vertex-pointed maps (as obtained for instance via $[t^n](2R+S^2)/(2n)$). This leads to the following expressions for the average numbers of edges of type $(i-1,i)$, (i,i)

and $(i+1,i)$, respectively

$$\begin{aligned} e_{i-1,i} &= \frac{3}{2}(\delta_i - \delta_{i-1}) \\ &= \frac{i(i+3)(2i+3)\left(5i^4+30i^3+67i^2+66i+28\right)}{35(i+1)^2(i+2)^2}, \\ e_{i,i} &= \frac{3}{2}(\eta_i - \eta_{i-1}) \\ &= \frac{2\mathfrak{E}_i}{35(i+1)^2(i+2)(i+3)^2} \end{aligned}$$

with $\mathfrak{E}_i = 5i^8+80i^7+537i^6+1964i^5+4251i^4+5528i^3+4175i^2+1660i+280$,

$$\begin{aligned} e_{i+1,i} &= e_{i,i+1} \\ &= \frac{3}{2}(\delta_{i+1} - \delta_i) \\ &= \frac{(i+1)(i+4)(2i+5)(5i^4+50i^3+187i^2+310i+196)}{35(i+2)^2(i+3)^2}, \end{aligned}$$

for $i \geq 0$. We have in particular an average number $e_{0,1} = 28/9$ (resp. $e_{0,0} = 8/9$) of half edges incident to the pointed vertex whose complementary half edge is incident to a distinct (resp. the same) vertex. These two numbers add up to 4, as expected since a large map has asymptotically 4 times more half edges than vertices. From the singularity

$$\log(R_i)|_{\text{sing.}} \sim (1-12t)^{3/2}\theta_i$$

we easily deduce the average number of vertices at distance i from the pointed vertex in infinitely large vertex-pointed maps:

$$v_i = \frac{3}{2}(\theta_i - \theta_{i-1}) = \frac{3}{280}(2i+3)(10i^2+30i+9), \quad \text{for } i \geq 1.$$

3.2. The two-point function of bipartite maps. We may now easily play the same game with general *bipartite* maps, which, upon blowing their edges into dark faces of degree 2, are nothing but general 2-constellations.

3.2.1. Computation from the bijective approach. Considering a pointed rooted bipartite map, its root edge is now necessarily of type $(j-1,j)$ or $(j+1,j)$ for some j. We use the same notation $R_i \equiv R_i(t)$ to now denote the generating function of pointed rooted bipartite maps enumerated with a weight t per edge, whose root edge is of type $(j-1,j)$ for $j \leq i$. This is also the generating function for vertex-pointed and rooted 2-constellations, with a weight t per dark face, and a root face of ccw-type $\tau = (j, j-1)$ for $j \leq i$ if we endow the constellation with its geodesic labeling.

From Proposition 3, the later are in one-to-one correspondence with 2-descending mobiles with a marked black vertex of cw-type $\overline{\tau}^{\uparrow} = (j, j+1)$, $j \leq i$.

Denoting $T_i = T_i(t)$ the generating function of floating (i.e., with arbitrary positive minimal label) 2-descending mobiles planted at a white vertex labeled i, enumerated with a weight t per black vertex, we deduce immediately the same identification as before

$$R_i = 1 + t\,T_i\,T_{i+1} \quad i \geq 1. \tag{8}$$

The generating function T_i is now obtained by solving the equation

$$T_i = \frac{1}{1 - t\,(T_{i-1} + T_{i+1})}, \quad i \geq 1$$

with initial condition $T_0 = 0$, and one finds [6]

$$T_i = T\,\frac{(1-y^i)(1-y^{i+4})}{(1-y^{i+1})(1-y^{i+3})}, \quad \text{where } T = 1 + 2tT^2 \text{ and } y + \frac{1}{y} = \frac{1}{tT^2}. \tag{9}$$

This leads, after simplification, to

$$R_i = R\,\frac{(1-y^{i+1})(1-y^{i+4})}{(1-y^{i+2})(1-y^{i+3})}, \quad \text{where } R = 1 + tT^2.$$

We may also compute along the same lines as before the generating function V_i for vertex-pointed bipartite maps, enumerated with a weight t per edge, with an extra marked vertex at distance $j \leq i$ from the pointed vertex, with $i \geq 1$. Following the same chain of arguments as above, we have

$$\begin{aligned} V_i &= \sum_{k\geq 1} \frac{(t\,(T_{i-1} + T_{i+1}))^k}{k} - \sum_{k\geq 1} \frac{(t\,T_{i-1})^k}{k} \\ &= \log\Big(\frac{1 - t\,T_{i-1}}{1 - t\,(T_{i-1} + T_{i+1})}\Big) \\ &= \log(T_i\,(1 - t\,T_{i-1})) \\ &= \log(1 + t\,T_i\,T_{i+1}) \\ &= \log(R_i), \end{aligned}$$

valid for $i \geq 1$. Note that the relation between V_i and R_i is unchanged when going from general to bipartite maps. It holds for all classes of maps and hypermaps described here, as a consequence of the general BDG bijection; see [7], p. 12 and p. 21.

3.2.2. Comparison with the continued fraction approach. Again, part of this result may be re-derived from the approach of [8] by noting that enumerating bipartite maps with weight t per edge amounts to enumerating bipartite maps with unbounded even face degrees and with a weight t^k per $2k$-valent face. The generating function R is obtained in this framework via

$$R = 1 + \sum_{k\geq 1} t^k \binom{2k-1}{k-1} R^k = \frac{1+\sqrt{1-4tR}}{2\sqrt{1-4tR}}; \tag{10}$$

namely

$$R = \frac{1-\sqrt{1-8t}+4t}{8t}.$$

This expression is compatible with $R = 1 + tT^2$ for

$$T = \frac{1-\sqrt{1-8t}}{4t}$$

which is the solution of $T = 1 + 2tT^2$, as wanted. For bipartite maps, the generating function R_i is now expected to take the form [5]

$$R_i = R\frac{u_i u_{i+3}}{u_{i+1}u_{i+2}} \tag{11}$$

and the characteristic equation reads

$$\begin{aligned} 1 &= \sum_{k=1}^{\infty} t^k R^{k-1} \sum_{q=0}^{k-1} \binom{2k-2-2q}{k-1-q} \Big(x+\frac{1}{x}\Big)^{2q} \\ &= \frac{t(1-4tR)^{-1/2}}{1-tR\Big(x+\dfrac{1}{x}\Big)^2}. \end{aligned}$$

Setting $R = 1 + tT^2$ and using $T = 1 + 2tT^2$, this simplifies into

$$x^2 + \frac{1}{x^2} = \frac{1}{tT^2}$$

which again allows us to identify $x^2 = y$ and deduce the simple form

$$u_i = c\lambda^i(1-x^{2i+2})$$

for some c and λ. Getting this expression for u_i via the continued fraction approach is still an open question.

3.2.3. Applications. Again, we may compute the average number of edges of type $(i-1,i)$ or $(i+1,i)$ in an infinitely large vertex-pointed bipartite map, as well as the average number of vertices at distance i. We find

$$e_{i-1,i} = \frac{2i(i+4)(10i^4+80i^3+233i^2+292i+141)}{105(i+1)(i+2)(i+3)}$$

and

$$\begin{aligned} e_{i+1,i} &= e_{i,i+1} \\ &= \frac{2(i+1)(i+5)(10i^4+120i^3+533i^2+1038i+756)}{105(i+2)(i+3)(i+4)}, \end{aligned}$$

for $i \geq 0$, and

$$v_i = \frac{4}{315}(i+2)(10i^2+40i+13),$$

for $i \geq 1$. We have in particular an average number $e_{0,1} = 3$ of half edges incident to the pointed vertex, as expected since a large bipartite map has asymptotically 3 times more half edges than vertices (this is easily seen from the "trivial" bijection between bipartite maps and Eulerian triangulations).

3.2.4. The two-point functions of general hypermaps. The recourse to 2-descending mobiles used above for the computation of the two-point function of bipartite maps turns out to be also helpful to compute the two-point function of general hypermaps. Recall that in vertex-pointed hypermaps, each vertex v is labeled by the length of a shortest path from the pointed vertex to v and having only dark faces to its right. Upon using Remark 4, it can be shown that the generating function $\mathcal{R}_i = \mathcal{R}_i(t)$ of vertex-pointed general hypermaps with a marked edge of type $(j-1,j)$ for $j \leq i$ (hence with a dark face on the right of the edge), enumerated with a weight t per edge of the hypermap, is identical to that of 2-descending mobiles with a marked triple of consecutive white labeled vertices of labels $(j, j+1, j+2)$ with $j \leq i$, with a weight t per black vertex. A proof of this statement is given just below. The two-point function $\mathcal{R}_i$ therefore reads

$$\mathcal{R}_i = 1 + t^2 T_i T_{i+1} T_{i+2}, \tag{12}$$

$i \geq 1$, with T_i as in (9) (again we incorporate in $\mathcal{R}_i$ a conventional term 1). Using the explicit form of T_i, we immediately deduce the factorized form

$$\mathcal{R}_i = \mathcal{R}\frac{(1-y^{i+2})(1-y^{i+4})}{(1-y^{i+3})^2} \quad \text{where } \mathcal{R} = 1 + t^2 T^3.$$

As for vertex-pointed general hypermaps with a marked edge of a type different from $(j-1,j)$, we have no simple expression for their generating function. Equation (12) is a consequence of the following claim.

Claim 6. *In the bijection of Remark 4 between vertex-pointed hypermaps (endowed with their geodesic labeling) and 2-descending mobiles, each edge $(i-1,i)$ of the hypermap corresponds to a triple of consecutive white labeled vertices of labels $(i,i+1,i+2)$ in counterclockwise order around the mobile. And the vertex of label i of the edge identifies to the vertex of label i of the triple.*

Proof. Recall that the bijection can be seen as the composition of 3 correspondences, see Figure 16: (1) between vertex-pointed hypermaps and vertex-pointed bipartite maps (Proposition 2), (2) between vertex-pointed bipartite maps and vertex-pointed stretched quadrangulations, (3) between vertex-pointed stretched quadrangulations and 2-descending mobiles (the composition of (2) and (3) corresponding to Proposition 3, upon identifying bipartite maps with 2-constellations).

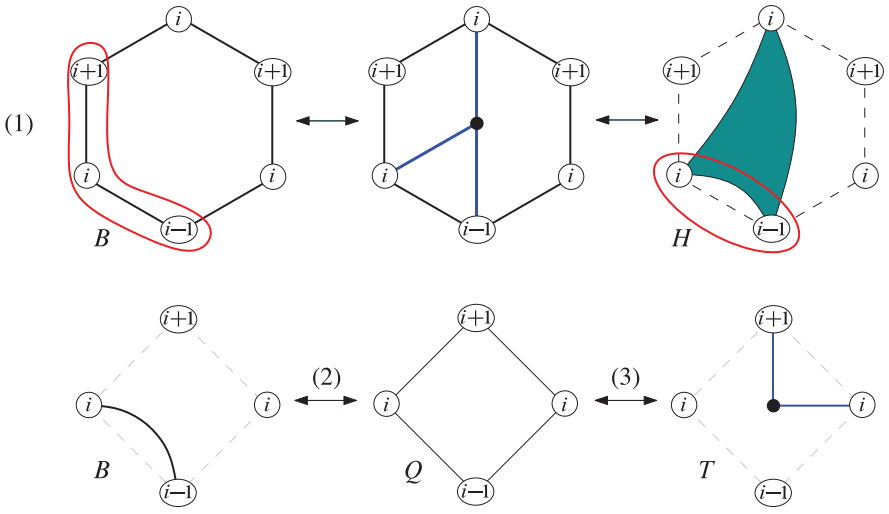

Figure 16. Local rules for the correspondence between a vertex-pointed hypermap H and a 2-descending mobile T, via a vertex-pointed bipartite map B and a vertex-pointed stretched quadrangulation Q. The top-line shows that an edge $(i-1,i)$ of H corresponds to a consecutive triple $(i-1,i,i+1)$ in clockwise order around a face of B.

We have to study how an edge $(i-1,i)$ of the hypermap is transported through each of the 3 steps. Given the local rules of Φ^- (see Figure 16), it is clear that each edge $(i-1,i)$ of a vertex-pointed hypermap corresponds to a triple of consecutive vertices of labels $(i-1,i,i+1)$ in clockwise order around a face of the associated vertex-pointed bipartite map. To look at the parameter-correspondence in steps (2) and (3) we find it simpler to take the point of view of stretched quadrangulations. Let Q be a vertex-pointed stretched quadrangulation, B the corresponding vertex-pointed bipartite map. Each non local max vertex v of label i in Q identifies to a vertex of label i in B. By the local rules of Φ^-, a corner c of Q at v yields an edge e of B

incident to v if and only if the neighbor (in Q) of v on the left side of c has label $i+1$, and in that case the other extremity of e has same label as the neighbor (in Q) of v on the right side of c. It easily follows that each clockwise-consecutive triple $(i-1, i, i+1)$ in B corresponds in Q to a vertex v of label i together with a triple of (clockwise) consecutive neighbors of v of labels $(i+1, i+1, i-1)$. Regarding Q, define an $(i-1)$-sector of v as a corner at v upon removing the edges $(i, i+1)$ around v; note that clockwise-consecutive triples of neighbors of labels $(i+1, i+1, i-1)$ around v are in 1-to-1 correspondence with $(i-1)$-sectors (around v) of multiplicity strictly larger than 1 (the multiplicity being the number of removed $(i, i+1)$ edges). Now we can discuss step (3) of the bijection. Let T be the 2-descending mobile associated to Q. By the local rules of Φ, each $(i-1)$-sector s at v yields exactly one edge of T (in the first corner in clockwise order around the sector). In addition, as shown in Figure 17, this edge leads to a white vertex w of label $i-1$ (resp. $i+1$) if s has multiplicity 0 (resp. >0), and in the second case the next vertex after w (in counterclockwise order around the mobile) has label i (resp. $i+2$) if s has multiplicity 1 (resp. >1). This concludes the proof. □

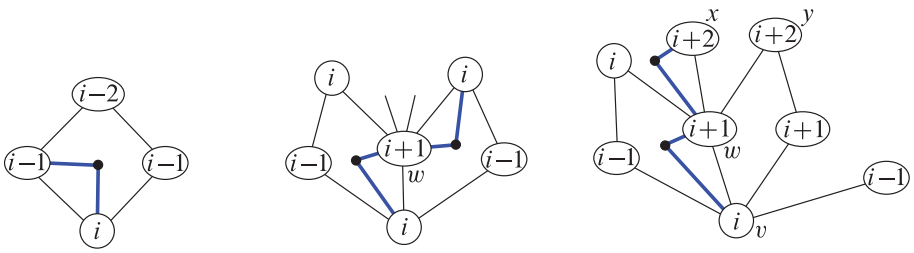

Figure 17. The 3 cases for an $(i-1)$-sector at a vertex of label i in Q: multiplicity 0, 1 and ≥ 2, respectively. The second case can take the degenerated form where the faces on each side of the edge $(i, i+1)$ are the same, in which case w is a leaf of the 2-descending mobile. In the third case, the successor of w of label $i+2$ around the mobile is generically defined as the unique neighbor x of w such that the neighbor preceding x (in clockwise order around w) has label i and all neighbors of w between x and y have label $i+2$.

3.3. The two-point function of 3-hypermaps. Consider now a vertex-pointed and rooted 3-hypermap (recall that the root edge is oriented so as to have the dark incident face – the root face – on its right). We wish to enumerate such 3-hypermaps endowed with their geodesic labeling and with their root face of ccw-type (j_1, j_2, j_3). By convention, when giving the type of the root face, we shall always start the cyclic sequence from the endpoint of the root edge (in particular, the root edge has its origin and endpoint at respective distances j_2 and j_1 from the pointed vertex). Note that the only possible ccw-types for the root face are of the form $(j, j-1, j-2)$, $(j, j-1, j-1)$, $(j, j-1, j)$, $(j, j-1, j+1)$, $(j, j, j-1)$, (j, j, j), $(j, j, j+1)$, $(j, j+1, j)$, $(j, j+1, j+1)$ and $(j, j+2, j+1)$ for some j. We call $R_{i_1,i_2,i_3} = R_{i_1,i_2,i_3}(t)$

the generating function for vertex-pointed and rooted 3-hypermaps, enumerated with a weight t per dark face, whose root face is of ccw-type $\tau = (i_1 - m, i_2 - m, i_3 - m)$ for some $m \geq 0$ (clearly $m \leq \min(i_1, i_2, i_3)$ by definition and the allowed values of (i_1, i_2, i_3) have the same form as the ccw-types listed above). Note that, in a 3-hypermap, the number of edges is three times the number of dark faces, so our counting amounts to attaching a weight $t^{1/3}$ to each edge.

From Theorem 2, these 3-hypermaps are in one-to-one correspondence with 3-mobiles with a marked black vertex of cw-type $\overline{\tau}^{\uparrow}$, one of its incident half-edges being distinguished. Note that the labels encountered in the sequence $\overline{\tau}^{\uparrow}$ are precisely $i_1 - m + 1$, $i_2 - m + 1$ and $i_3 - m + 1$ (with a prescribed order of appearance). Hence, gathering all cases for all $m \geq 0$ and shifting the labels by m, we end up with floating 3-mobiles with a marked black vertex adjacent to white vertices with labels $i_1 + 1$, $i_2 + 1$ and $i_3 + 1$ in a prescribed order. This allows to write, for the allowed values of (i_1, i_2, i_3)

$$R_{i_1,i_2,i_3} = t T_{i_1+1} T_{i_2+1} T_{i_3+1}$$

where T_i is the generating function of floating 3-mobiles planted at a white vertex with label i. This later generating function is easily shown to satisfy

$$T_i = \frac{1}{1 - \mathfrak{T}_i},$$

where

$$\mathfrak{T}_i = t(T_{i-2}T_{i-1} + T_{i-1}^2 + 2T_{i-1}T_i + T_i^2 + T_{i-1}T_{i+1} + 2T_iT_{i+1} + T_{i+1}^2 + T_{i+1}T_{i+2}),$$

for $i \geq 1$ with initial conditions $T_0 = 0$ and $T_{-1}T_0 = 0$. This equation expresses that a floating 3-mobiles planted at a white vertex labeled i may be viewed as a sequence of pairs of planted floating 3-mobiles – attached to the root vertex via trivalent black vertices – with appropriate root labels. As explained in [5], Section 6.1, and in [8], we have the explicit formula

$$T_i = T \frac{v_i(y_1, y_2) v_{i+3}(y_1, y_2)}{v_{i+1}(y_1, y_2) v_{i+2}(y_1, y_2)}, \quad \text{where } T = 1 + 10tT^3.$$

Here y_1 and y_2 are the two solutions (with modulus less than 1) of

$$y^2 + 6y + 6 + \frac{6}{y} + \frac{1}{y^2} = \frac{1}{tT^3}$$

(note that, in particular y_1 and y_2 are related by $y_1 + y_1^{-1} + y_2 + y_2^{-1} + 6 = 0$) and $v_i(y_1, y_2)$ denotes

$$v_i(y_1, y_2) = 1 - \frac{1 - y_1 y_2}{y_1 - y_2} y_1^{i+1} - \frac{1 - y_1 y_2}{y_2 - y_1} y_2^{i+1} - y_1^{i+1} y_2^{i+1}.$$

Consider now a vertex-pointed and rooted 3-hypermap and concentrate on the type of its root edge, defined as the pair (k, j) of the respective distances of its origin

and of the endpoint from the pointed vertex. In particular, we denote as in previous sections by $R_i \equiv R_i(t), i \geq 1$ the generating function for vertex-pointed and rooted 3-hypermaps with a root edge is of type $(j-1, j)$ for $j \leq i$. Listing the possible corresponding ccw-type of the root face, namely $(j, j-1, j-2)$, $(j, j-1, j-1)$, $(j, j-1, j)$ or $(j, j-1, j+1)$, we deduce

$$\begin{aligned} R_i &= 1 + R_{i+1,i,i-1} + R_{i+1,i,i} + R_{i+1,i,i+1} + R_{i+1,i,i+2} \\ &= 1 + t\,T_i T_{i+1}(T_{i-1} + T_i + T_{i+1} + T_{i+2}) \end{aligned}$$

with, as before, a conventional term 1. After some tedious calculations, we find, using the above mentioned relation between y_1 and y_2, the remarkable simplification

$$R_i = R\frac{v_{i+1}(y_1, y_2)v_{i+3}(y_1, y_2)}{(v_{i+2}(y_1, y_2))^2} \quad \text{where } R = 1 + 4tT^3.$$

We may finally compute the generating function V_i for vertex-pointed 3-hypermaps, enumerated with a weight t per dark face, with an extra marked vertex at distance $j \leq i$ from the pointed vertex, with $i \geq 1$ (again with their symmetry factor). From Proposition 3, V_i is the generating function for floating 3-mobiles with a marked non-right-local-max vertex labeled i and we may write

$$\begin{aligned} V_i &= \sum_{k\geq 1} \frac{\mathfrak{T}_i^k - (t(T_{i-2}T_{i-1} + T_{i-1}^2 + 2T_{i-1}T_i + T_i^2 + T_iT_{i+1}))^k}{k} \\ &= \log(T_i(1 - t(T_{i-2}T_{i-1} + T_{i-1}^2 + 2T_{i-1}T_i + T_i^2 + T_iT_{i+1}))) \\ &= \log(1 + t\,T_iT_{i+1}(T_{i-1} + T_i + T_{i+1} + T_{i+2})) \\ &= \log(R_i), \end{aligned}$$

valid for $i \geq 1$ (the subtracted term removes configurations where the root vertex would be a right-local max). We thus recover the same relation $V_i = \log(R_i)$ as in previous sections, as expected.

3.4. The two-point function of 3-constellations. Consider finally vertex-pointed and rooted 3-constellations endowed with their geodesic labeling, whose root face is of ccw-type $(i_1 - m, i_2 - m, i_3 - m)$ for some $m \geq 0$ and denote again by $R_{i_1,i_2,i_3} = R_{i_1,i_2,i_3}(t)$ their generating function. The possible values of (i_1, i_2, i_3) are now restricted to $(i, i-1, i-2)$, $(i, i-1, i+1)$ and $(i, i+2, i+1)$ for some i.

3.4.1. Computation from the bijective approach. From Proposition 3, vertex-pointed and rooted 3-constellations with root face of ccw-type τ are in one-to-one correspondence with 3-descending mobiles with a marked black vertex of cw-type $\overline{\tau}^{\uparrow}$, one of its incident half-edges being distinguished. By the same argument as before, we find

$$R_{i_1,i_2,i_3} = t\,T_{i_1+1}T_{i_2+1}T_{i_3+1}$$

for the allowed values of (i_1, i_2, i_3). Here T_i denotes the generating function for floating 3-descending mobiles planted at a white vertex labeled i. It satisfies

$$T_i = \frac{1}{1 - t(T_{i-2}T_{i-1} + T_{i-1}T_{i+1} + T_{i+1}T_{i+2})}$$

for $i \geq 1$ with initial conditions $T_0 = 0$ and $T_{-1}T_0 = 0$. The solution of this equation was found (in the context of Eulerian quadrangulations viewed as a particular case of 4-constellations; see [5] and [12]) to be

$$T_i = T\frac{v_i(y_1, y_2)v_{i+5}(y_1, y_2)}{v_{i+1}(y_1, y_2)v_{i+4}(y_1, y_2)}, \quad \text{where } T = 1 + 3tT^3.$$

Here y_1 and y_2 are the two solutions (with modulus less than 1) of

$$y^2 + 2y + \frac{2}{y} + \frac{1}{y^2} = \frac{1}{tT^3}$$

(note that, in particular y_1 and y_2 are related by $y_1 + y_1^{-1} + y_2 + y_2^{-1} + 2 = 0$) and $v_i(y_1, y_2)$ now denotes

$$v_i(y_1, y_2) = 1 - \frac{p_1 - y_1^4 p_2}{p_1 - p_2}y_1^i - \frac{p_2 - y_2^4 p_1}{p_2 - p_1}y_2^i + \frac{y_2^4 p_1 - y_1^4 p_2}{p_1 - p_2}y_1^i y_2^i,$$

where

$$p_1 = y_1 + y_1^2 + y_1^3 \quad \text{and} \quad p_2 = y_2 + y_2^2 + y_2^3.$$

We may as before concentrate on the type of the root edge only and look for instance at the generating function $R_i \equiv R_i(t)$, $i \geq 1$ for vertex-pointed and rooted 3-constellations with a root edge of type $(j-1, j)$ for $j \leq i$. By listing the possible ccw-type of the root face, namely $(j, j-1, j-2)$ and $(j, j-1, j+1)$, we obtain

$$\begin{aligned} R_i &= 1 + R_{i+1,i,i-1} + R_{i+1,i,i+2} \\ &= 1 + tT_iT_{i+1}(T_{i-1} + T_{i+2}) \end{aligned}$$

with, as before, a conventional term 1. We find the remarkable simplification

$$R_i = R\frac{v_{i+1}(y_1, y_2)v_{i+5}(y_1, y_2)}{v_{i+2}(y_1, y_2)v_{i+4}(y_1, y_2)}, \quad \text{where } R = 1 + 2tT^3.$$

We may as before evaluate the generating function V_i for vertex-pointed 3-constellations, enumerated with a weight t per dark face, with an extra marked vertex at distance $j \leq i$ from the pointed vertex, with $i \geq 1$ (with symmetry factors). Repeating the arguments of previous Sections, we again have the relation $V_i = \log(R_i)$.

3.4.2. Comment on the form of the two-point function. Let us now comment on the respective forms of T_i and R_i: first we note that the indices involved in the respective bi-ratios of v's match what we expect for constellations. As discussed in [5], and in [12], we expect the two-point function for pointed rooted p-constellations to display a bi-ratio of the form $(U_i/U_{i+1})/(U_{i+p}/U_{i+p+1})$. The observed form of T_i is thus typical of 4-constellations (with $U_i \longleftrightarrow v_i$) in agreement with the fact that, from the BDG bijection, T_i may be interpreted as a two-point function for 4-regular constellations (i.e., Eulerian quadrangulations). As for the form of R_i, it is typical of 3-constellations (with $U_i \longleftrightarrow v_{i+1}$) as it should. A second remark concerns the precise value of the function $v_i(y_1, y_2)$. Its observed form is characteristic of 4-constellations while, for a 3-constellation, one would have expected instead in [5] and in [12]

$$v_i(y_1, y_2) = 1 - \frac{p_1' - y_1^3 p_2'}{p_1' - p_2'} y_1^i - \frac{p_2' - y_2^3 p_1'}{p_2' - p_1'} y_2^i + \frac{y_2^3 p_1' - y_1^3 p_2'}{p_1' - p_2'} y_1^i y_2^i,$$

where

$$p_1' = y_1 + y_1^2, \quad \text{and} \quad p_2' = y_2 + y_2^2.$$

Remarkably enough, the two expressions do coincide whenever $y_1 + y_1^{-1} + y_2 + y_2^{-1} + 2 = 0$, which is precisely the above mentioned condition satisfied by y_1 and y_2 in the solution for T_i. In other words, the observed form for $v_i(y_1, y_2)$ matches both that expected for 4-constellations and that expected for 3-constellations, a non-trivial property. Note that the relation between y_1 and y_2 (and therefore the coincidence of the two expressions for v_i) holds only when dealing with a very specific family of 4-constellations, namely the 4-regular ones.

This property generalizes as follows: the expected form for the two-point function R_i for a p-constellation is (see [5] and [12])

$$R_i = R \frac{v_i v_{i+p+1}}{v_{i+1} v_{i+p}}$$

where $v_i = v_i(y_1, y_2, \cdots, y_m)$ takes the form

$$v_i(y_1, y_2, \cdots, y_m) = \sum_{I \subset \{1,2,\cdots,m\}} \prod_{k \in I} \lambda_k y_k^i \prod_{k,k' \in I} \frac{(p_k^{(p)} - p_{k'}^{(p)})(q_k^{(p)} - q_{k'}^{(p)})}{(p_k^{(p)} - q_{k'}^{(p)})(q_k^{(p)} - p_{k'}^{(p)})}.$$

Here the sum is over all subsets I of $\{1, 2, \cdots, m\}$. The quantities y_i are the solutions (with modulus less than one) of a characteristic equation depending on the problem at hand (and their number m depends on the problem too) and the λ_k are fixed by demanding $v_0 = v_1 = v_{-2} = \cdots = v_{-m+1} = 0$. Finally, $p_k^{(p)}$ and $q_k^{(p)}$ are defined as

$$p_k^{(p)} = y_k + y_k^2 + \cdots + y_k^{p-1} \quad \text{and} \quad q_k^{(p)} = y_k^{-1} + y_k^{-2} + \cdots + y_k^{-p+1}.$$

The reader will easily check that all the specific expressions given above for 2-, 3-, and 4-constellations are indeed of this form. Now, from our bijections, the two-point function R_i in the case of p-constellations enumerated with a weight t per dark face is easily expressed in terms of the generating function T_i for descending p-mobiles with a weight t per black vertex, which is itself the two-point function for a particular instance of $(p+1)$-constellations, namely $(p+1)$-regular constellations (i.e., with all their dark and light faces of degree $(p+1)$), enumerated with a weight t per dark face. As such, T_i takes the form expected for a $(p+1)$-constellation (with moreover $m = p-1$ in this case)

$$T_i = T\frac{v_i v_{i+p+2}}{v_{i+1}v_{i+p+1}}$$

(with T solution of $T = 1 + tpT^p$ in this case) where $v_i = v_i(y_1, y_2, \cdots, y_{p-1})$ now reads

$$v_i(y_1, y_2, \cdots, y_{p-1}) = \sum_{I\subset\{1,2,\cdots,p-1\}} \prod_{k\in I} \lambda_k y_k^i \prod_{k,k'\in I} \frac{(p_k^{(p+1)} - p_{k'}^{(p+1)})(q_k^{(p+1)} - q_{k'}^{(p+1)})}{(p_k^{(p+1)} - q_{k'}^{(p+1)})(q_k^{(p+1)} - p_{k'}^{(p+1)})}.$$

The reader may again check that the specific expressions given above for 3- and 4-regular constellations are indeed of this form. It is tempting to conjecture that the v_i appearing in R_i is the same as that appearing in T_i (we have seen above that this holds for $p = 2$ and $p = 3$) and that the precise relation between R_i and T_i is responsible for the change of indices in the involved bi-ratios. As a check of consistency for this conjecture to hold for general p, we can verify that $v_i(y_1, y_2, \cdots, y_{p-1})$, as given just above, may be rewritten in the form expected for a p-constellation, which requires, for all pairs $\{y_k, y_{k'}\}$ of distinct solutions of the characteristic equation for $(p+1)$-regular constellations,

$$\frac{(p_k^{(p+1)} - p_{k'}^{(p+1)})(q_k^{(p+1)} - q_{k'}^{(p+1)})}{(p_k^{(p+1)} - q_{k'}^{(p+1)})(q_k^{(p+1)} - p_{k'}^{(p+1)})} = \frac{(p_k^{(p)} - p_{k'}^{(p)})(q_k^{(p)} - q_{k'}^{(p)})}{(p_k^{(p)} - q_{k'}^{(p)})(q_k^{(p)} - p_{k'}^{(p)})}. \tag{13}$$

The later reads explicitly

$$H(y) \equiv \sum_{k=1}^{p-1}(p-k)\Big(y^k + \frac{1}{y^k}\Big) = \frac{1}{tT^p}, \quad \text{where } T = 1 + ptT^p.$$

To prove (13), we note, using $y_k^p q_k^{(p)} = p_k^{(p)}$, that

$$\frac{(p_k^{(p)} - p_{k'}^{(p)})(q_k^{(p)} - q_{k'}^{(p)})}{(p_k^{(p)} - q_{k'}^{(p)})(q_k^{(p)} - p_{k'}^{(p)})} = \frac{a_{kk'}^{(p)} + a_{k'k}^{(p)} - 1}{a_{kk'}^{(p)} a_{k'k}^{(p)}}$$

where

$$a_{kk'}^{(p)} = \frac{y_{k'}^p p_k^{(p)} - p_{k'}^{(p)}}{p_k^{(p)} - p_{k'}^{(p)}}$$

so (13) is satisfied if $a_{kk'}^{(p)} = a_{kk'}^{(p+1)}$, or equivalently

$$\begin{aligned} 0 &= (y_{k'}^p p_k^{(p)} - p_{k'}^{(p)})(p_k^{(p+1)} - p_{k'}^{(p+1)}) - (y_{k'}^{p+1} p_k^{(p+1)} - p_{k'}^{(p+1)})(p_k^{(p)} - p_{k'}^{(p)}) \\ &= (y_k y_{k'})^p (1 - y_{k'})(H(y_k) - H(y_{k'})), \end{aligned}$$

which holds precisely whenever y_k and $y_{k'}$ are two solutions of the characteristic equation, since $H(y_k) = H(y_{k'})$ in this case. That the passage from T_i to R_i induces the wanted change of indices in the involved bi-ratios of v_i is far from obvious and we have not found any simple argument that would explain this property for general p.

4. Two-point functions depending on two parameters

So far, we have not exploited the full power of the bijection of Theorem 2, and in particular the property that it transforms the faces of a (hyper)map into right local max of the corresponding mobile. In this section, we will use this property in order to derive the two-point function of general planar maps and bipartite planar maps counted according to *two size parameters*: the number of edges and the number of faces. (Note that the number of vertices is then fixed by Euler's relation.)

The case of general planar maps was actually first treated in [1], Section 5, but we will recall its derivation for completeness.

4.1. The two-point function of general maps with edge and face weights. Our purpose is to obtain a generalization of the two-point function of general maps derived in Section 3.1 depending on two formal variables: the previous weight t per edge, and an extra weight z per face. We still denote by $R_i \equiv R_i(t,z)$, $i \geq 1$ (resp. $S_i^2 \equiv S_i(t,z)^2$, $i \geq 0$) the generating function of pointed rooted maps whose root edge is of type $(j-1, j)$ (resp. (j, j)) for $j \leq i$.

By Theorem 2, these generating functions may alternatively be understood as counting some floating 2-mobiles, and the variable z now plays the role of a weight per right local max. Note that, upon removing the bivalent black vertices, a right local max is nothing but a vertex having no neighbor with strictly larger label. We still denote by $T_i \equiv T_i(t,z)$ the generating function of floating 2-mobiles planted at a white vertex labeled i, with this extra variable. In order to extend (2) to the case $z \neq 1$, we shall introduce another generating function $U_i \equiv U_i(t,z)$ counting the same objects, but where the root vertex does not receive the weight z if it is a

local max. We then have the equations

$$T_i = z + t(T_i U_{i-1} + T_i^2 + U_i T_{i+1}), \tag{14a}$$

$$U_i = 1 + t(U_i U_{i-1} + U_i T_i + U_i T_{i+1}), \tag{14b}$$

with initial data $T_0 = U_0 = 0$, which are obtained by a straightforward recursive decomposition. Clearly, these equations admit a unique solution in the set of sequences of formal power series in t and z.

Ambjørn and Budd derived these equations in a slightly different form and, remarkably, found an exact expression for their solution. It takes the form of equation (26) in [1]

$$T_i = T\frac{(1-y^i)(1-\alpha^2 y^{i+3})}{(1-\alpha y^{i+1})(1-\alpha y^{i+2})}, \tag{15a}$$

$$U_i = U\frac{(1-y^i)(1-\alpha y^{i+3})}{(1-y^{i+1})(1-\alpha y^{i+2})}, \tag{15b}$$

where T, U, y and α may be determined by the condition that this ansatz satisfies the equations. In practice, substituting (15) into (14) yields a system of two equations of the form

$$P_s(t, z, T, U, y, \alpha, y^i) = 0, \quad s = 1, 2, \tag{16}$$

where P_1, P_2 are seven-variable polynomials that are independent of i. Thus, expanding P_1, P_2 with respect to the last variable, all the coefficients should vanish identically, which yields a system of algebraic equations relating t, z, T, U, y, α. Miraculously, this system defines a two-dimensional variety, which allows to determine the "unknowns" T, U, y, α as algebraic power series in the variables t and z. Of course, we find that T and U are nothing but the constant solutions of (14), namely they are specified by the tree equations

$$T = z + t(T^2 + 2TU), \tag{17a}$$

$$U = 1 + t(2TU + U^2), \tag{17b}$$

while we find that y and α are obtained by inverting the relations

$$t = \frac{y(1-\alpha y)^3(1-\alpha y^3)}{(1+y+\alpha y-6\alpha y^2+\alpha y^3+\alpha^2 y^3+\alpha^2 y^4)^2}, \tag{18a}$$

$$z = \frac{\alpha(1-y)^3(1-\alpha^2 y^3)}{(1-\alpha y)^3(1-\alpha y^3)}. \tag{18b}$$

The first few terms of y and α read

$$y = t + (2+5z)t^2 + (5+31z+23z^2)t^3 + (14+153z+275z^2+102z^3)t^4 + \ldots$$

and

$$\alpha = z + 3z(1-z)t + 3z(1-z)(4+z)t^2 + z(1-z)(49+51z+4z^2)t^3 + \dots,$$

and it can be shown that y and α are indeed series in t whose coefficients are polynomials in z with integer coefficients. Furthermore, it appears that all coefficients of y and αy are nonnegative, which suggests a possible combinatorial interpretation. For bookkeeping purposes, let us mention the nice relations

$$\frac{U}{T} = \frac{(1-\alpha y)^2}{\alpha(1-y)^2}$$

and

$$tT^2 = \frac{\alpha^2 y(1-y)^4}{(1-\alpha y)^3(1-\alpha y^3)}.$$

Recalling now the actual mobile interpretation of the generating functions R_i and S_i of Section 3.1, we easily obtain the expressions

$$R_i = 1 + tU_iT_{i+1}, \quad i \geq 1,$$
$$S_i = \sqrt{t}T_i, \qquad\qquad i \geq 0,$$

which extend (1) in the case $z \neq 1$. Interestingly, we find that R_i reads

$$R_i = R\frac{(1-\alpha y^{i+1})(1-\alpha y^{i+3})}{(1-\alpha y^{i+2})^2}$$

where

$$R = 1 + tUT = \frac{(1-\alpha y^2)^2}{(1-\alpha y)(1-\alpha y^3)},$$

which naturally matches the form (6) expected from the continued fraction approach, since our problem now amounts to considering maps with a weight $g_k = zt^{k/2}$ per face of degree k. As for S_i, it might also be written in the form (6), albeit in a non-unique manner. We might also repeat the exercise of Section 3.1.2 and check that R and $S = \sqrt{t}T$ satisfy the relations

$$S = z\sum_{k=1}^{\infty} t^{k/2}P(k-1, R, S), \tag{19a}$$

$$R = 1 + \frac{z}{2}\sum_{k=1}^{\infty} t^{k/2}P(k, R, S) - \frac{S^2}{2}, \tag{19b}$$

extending (7). Doing a full derivation of the two-point functions from the continued fraction approach is a challenging open question.

4.2. The two-point function of bipartite maps with edge and face weights. We may attempt the same approach in the case of bipartite maps, to obtain a two-variable generalization of the two-point function derived in Section 3.2. Let $R_i \equiv R_i(t,z)$, $i \geq 1$, be the generating function of pointed rooted bipartite maps whose root edge is of type $(j-1, j)$, $j \leq i$, counted with a weight t per edge and z per face. By Proposition 3, such maps are in bijection with some floating 2-descending mobiles, with z a weight per (right) local max. Denote again by $T_i \equiv T_i(t,z)$ (resp. $U_i \equiv U_i(t,z)$) the generating functions of floating 2-descending mobiles planted at a white vertex labeled i, counted with a weight t per black vertex and z per right local max (resp. right local max distinct from the root vertex). We now find the recursive decomposition equations

$$T_i = z + t(T_i U_{i-1} + U_i T_{i+1}), \tag{20a}$$

$$U_i = 1 + t(U_i U_{i-1} + U_i T_{i+1}), \tag{20b}$$

with initial data $T_0 = U_0 = 0$.

Inspired by the Ambjørn-Budd solution (15) for general maps and by the form (9) for $T_i = U_i$ at $z = 1$, we make the ansatz

$$T_i = T\frac{(1-y^i)(1-\alpha^2 y^{i+4})}{(1-\alpha y^{i+1})(1-\alpha y^{i+3})}, \tag{21a}$$

$$U_i = U\frac{(1-y^i)(1-\alpha y^{i+4})}{(1-y^{i+1})(1-\alpha y^{i+3})}. \tag{21b}$$

Repeating the same strategy as in the previous section we find, miraculously again, that there exists T, U, y and α which are algebraic power series in t and z such that the ansatz satisfies the equations. As expected T and U are specified by

$$T = z + 2tTU, \tag{22a}$$

$$U = 1 + tU(T+U), \tag{22b}$$

while y and α are obtained by inverting

$$t = \frac{y(1-\alpha y)^2(1-\alpha y^4)}{(1+y)^2(1-\alpha y^2)^3}, \tag{23a}$$

$$z = \frac{\alpha(1-y)^2(1-y^2)(1+\alpha y^2)}{(1-\alpha y)^2(1-\alpha y^4)}. \tag{23b}$$

We note that T and U are parametrized in terms of y and α by

$$T = \frac{\alpha(1-y^2)^2(1-\alpha y^2)}{(1-\alpha y)^2(1-\alpha y^4)}, \tag{24a}$$

$$U = \frac{(1+y)(1-\alpha y^2)^2}{(1-\alpha y)(1-\alpha y^4)} \tag{24b}$$

and that the first few terms of y and α read

$$y = t + 2(1+z)t^2 + (5+13z+3z^2)t^3 + (14+66z+40z^2+4z^3)t^4 + \dots,$$

and

$$\alpha = z + 2z(1-z)t + z(1-z)(8-z)t^2 + 32z(1-z)t^3 + \dots.$$

(It can again be shown that y and α are series in t whose coefficients are polynomials in z with integer coefficients, and it seems that all coefficients of y and αy are positive.)

By the mobile interpretation of R_i explained in Section 3.2, we have

$$R_i = 1 + tU_iT_{i+1}$$

which extends (8) for $z \neq 1$. We deduce that

$$R_i = R\frac{(1-\alpha y^{i+1})(1-\alpha y^{i+4})}{(1-\alpha y^{i+2})(1-\alpha y^{i+3})}$$

where

$$R = 1 + tUT = \frac{(1-\alpha y^2)(1-\alpha y^3)}{(1-\alpha y)(1-\alpha y^4)},$$

which matches the form (11) expected for the two-point function of a family of bipartite maps, according to the continued fraction approach (our weighting scheme is indeed equivalent to attaching a weight zt^k to each face of degree $2k$).

Finally, by a straightforward generalization of the arguments given in Section 3.2.4, we may compute the generating function $\mathcal{R}_i = \mathcal{R}_i(t,z)$ of vertex-pointed general hypermaps with a marked edge of type $(j-1, j)$ for $j \leq i$, enumerated now with both a weight t per edge of the hypermap and a weight z per dark face. It simply reads

$$\mathcal{R}_i = 1 + t^2U_iU_{i+1}T_{i+2}, \quad i \geq 1$$

(with as before a conventional term 1). Using the explicit form of T_i and U_i above, we arrive at the factorized form

$$\mathcal{R}_i = \mathcal{R}\frac{(1-\alpha y^{i+2})(1-\alpha y^{i+4})}{(1-\alpha y^{i+3})^2}$$

where

$$\mathcal{R} = 1 + t^2U^2T.$$

5. Conclusion

In this paper, we made extensive use of bijections to obtain the two-point function for a number of families of maps and hypermaps with unbounded faces degrees. We now list a few remarks and discuss possible extensions of our work, as well as open questions.

First, we have found that the two-point function R_i of general maps (resp. bipartite maps) counted by their number of edges is closely related to that of quadrangulations (resp. 3-regular constellations, i.e., Eulerian triangulations), counted by their number of faces (resp. dark faces). Indeed, we have $R_i = 1 + t\,T_i\,T_{i+1}$ where T_i, given by (3) (resp. (9)), and defined as a mobile generating function, can also be viewed as the two-point function for quadrangulations (resp. Eulerian triangulations), see [6]. As a consequence, it is easily checked that these quantities are the same in the scaling limit, namely the continuum two-point function $\varphi(r)$ of general maps (resp. bipartite maps)

$$\varphi(r) = \lim_{n\to\infty} \frac{[t^n]R_{\lfloor rn^{1/4}\rfloor}}{[t^n]R}$$

coincides with that of quadrangulations (resp. Eulerian triangulations), which reads explicitly [5]

$$\begin{aligned}\varphi(r) &= \lim_{n\to\infty} \frac{[t^n]T_{\lfloor rn^{1/4}\rfloor}}{[t^n]T} \\ &= \frac{4}{\sqrt{\pi}} \int_0^\infty d\xi\, \xi^2 e^{-\xi^2} \Big(1 - 6\frac{1-\cosh(ar\sqrt{\xi})\cos(ar\sqrt{\xi})}{(\cosh(ar\sqrt{\xi}) - \cos(ar\sqrt{\xi}))^2}\Big)\end{aligned}$$

with $a = \sqrt{3}$ (resp. $a = \sqrt{2}$). Recall that $\varphi(r)$ is known to coincide with the density of the supremum of the support of the Integrated Super-Brownian Excursion (ISE); see [11], [5], and [4]. Note that $\varphi(r)$ with $a = \sqrt{2}$ is also the continuum two-point function of general hypermaps $\varphi(r) = \lim_{n\to\infty} \frac{[t^n]\mathcal{R}_{\lfloor rn^{1/4}\rfloor}}{[t^n]\mathcal{R}}$. The equality of the two-point functions of general maps and quadrangulations in the scaling limit suggests the stronger property that these metric spaces are asymptotically the "same" (note that in both cases, the two-point function corresponds to the actual, symmetric, graph distance). Precisely, we conjecture that the Ambjørn-Budd bijection defines a coupling between uniform planar maps with n edges and uniform planar quadrangulations with n faces such that their Gromov-Hausdorff distance is asymptotically almost surely negligible with respect to $n^{1/4}$. Since the latter are known to converge to the Brownian map (see [15] and [13]), the convergence of the former would follow. (Addendum to the final version: this result has now been proved in [3].)

Second, we have shown that the two-point functions of general and bipartite maps match the form expected from the continued fraction approach. It would be interesting to have a full independent rederivation of our results via this approach. This requires the computation of Hankel determinants of growing size: in the context of maps with bounded face degrees; see [8], this was made through an identification of these determinants as symplectic Schur functions. Here no such reduction is available and this is therefore a challenging question.

Third, we have exhibited in Section 4 explicit expressions for the two-point functions of general maps and bipartite maps counted by both their number of edges and their number of faces. Our derivation makes use only of the case $p = 2$ of Theorem 2

and Proposition 3. It is natural to expect an extension of these formulas for general p, i.e., for p-hypermaps and p-constellations counted by both their number of dark faces and their number of light faces. In other words, we expect the system of equations satisfied by the corresponding 2-parameter generating functions to be still integrable. We have not however been able to guess its actual solution.

Returning to the case $p = 2$, the extra control on the number of faces allows to interpolate naturally between trees (maps with a single face) and arbitrary maps (with an unconstrained number of faces). For a fixed large number n of edges, the typical distance falls down from the known order $n^{1/2}$ for trees to $n^{1/4}$ for maps. We may then wonder about the possibility of obtaining new, non-generic, scaling limits for maps with "few" faces, where the distances would be of order n^{β} with $1/4 < \beta < 1/2$. We plan to investigate the question in the future.

References

[1] J. Ambjørn and T. G. Budd, Trees and spatial topology change in causal dynamical triangulations. *J. Phys. A* **46** (2013), Article Id. 315201, 33 pp. MR 3090757 Zbl 1273.81224

[2] J. Ambjørn and Y. Watabiki, Scaling in quantum gravity. *Nuclear Phys. B* **445** (1995), 129–142. MR 1338099 Zbl 1006.83015

[3] J. Bettinelli, E. Jacob, and G. Miermont, The scaling limit of uniform random plane maps, via the Ambjørn–Budd bijection. Preprint 2013. arXiv:1312.5842 [math.PR]

[4] M. Bousquet-Mélou, Limit laws for embedded trees: applications to the integrated super-Brownian excursion. *Random Structures Algorithms* **29** (2006), 475–523. MR 2268233 Zbl 1107.60302

[5] J. Bouttier, P. Di Francesco, and E. Guitter, Geodesic distance in planar graphs. *Nuclear Phys. B* **663** (2003), 535–567. MR 1987861 Zbl 1022.05022

[6] J. Bouttier, P. Di Francesco, and E. Guitter, Statistics of planar graphs viewed from a vertex: a study via labeled trees. *Nuclear Phys. B* **675** (2003), 631–660. MR 2018892 Zbl 1027.05021

[7] J. Bouttier, P. Di Francesco, and E. Guitter, Planar maps as labeled mobiles. *Electron. J. Combin.* **11** (2004), Article Id. 69, 27 pp. MR 2097335 Zbl 1060.05045

[8] J. Bouttier and E. Guitter, Planar maps and continued fractions. *Comm. Math. Phys.* **309** (2012), 623–662. MR 2885603 Zbl 1235.05067

[9] G. Chapuy, Asymptotic enumeration of constellations and related families of maps on orientable surfaces. *Combin. Probab. Comput.* **18** (2009), 477–516. MR 2507734 Zbl 1221.05204

[10] P. Chassaing and G. Schaeffer, Random planar lattices and integrated superBrownian excursion. *Probab. Theory Related Fields* **128** (2004), 161–212. MR 2031225 Zbl 1041.60008

[11] J.-F. Delmas, Computation of moments for the length of the one dimensional ISE support. *Electron. J. Probab.* **8** (2003), Article Id. 17, 15 pp. MR 2041818 Zbl 1064.60169

[12] P. Di Francesco, Geodesic distance in planar graphs: an integrable approach. *Ramanujan J.* **10** (2005), 153–186. MR 2194521 Zbl 1079.05040

[13] J.-F. Le Gall, Uniqueness and universality of the Brownian map. *Ann. Probab.* **41** (2013), 2880–2960. MR 3112934 Zbl 1282.60014

[14] G. Miermont, Tessellations of random maps of arbitrary genus. *Ann. Sci. Éc. Norm. Supér.* (4) **42** (2009), 725–781. MR 2571957 Zbl 1228.05118

[15] G. Miermont, The Brownian map is the scaling limit of uniform random plane quadrangulations. *Acta Math.* 210 (2013), 319–401. MR 3070569 Zbl 1278.60124

[16] G. Schaeffer, *Conjugaison d'arbres et cartes combinatoires aléatoires*. Ph.D. thesis, Université Bordeaux I, Bordeaux, 1998.

Communicated by Mireille Bousquet-Mélou

Received September 12, 2013; Accepted June 6, 2014

Jérémie Bouttier, Institut de Physique Théorique, CEA, IPhT, 91191 Gif-sur-Yvette, France, CNRS, URA 2306

Département de Mathématiques et Applications, École normale supérieure, 45 rue d'Ulm, 75231 Paris Cedex 05, France

E-mail: jeremie.bouttier@cea.fr

Emmanuel Guitter, Institut de Physique Théorique, CEA, IPhT, 91191 Gif-sur-Yvette, France, CNRS, URA 2306

E-mail: emmanuel.guitter@cea.fr

Éric Fusy, LIX, École Polytechnique, 91120 Palaiseau, France

E-mail: fusy@lix.polytechnique.fr